Final Report

Adsorption Equilibrium and Kinetics at Goethite-Water and Related Interfaces

Grant: DE-FG02-04ER15496

Submitted by

Dr. Lynn E. Katz

University of Texas at Austin

Department of Civil, Architectural and Environmental Engineering

Center for Research in Water and the Environment

Austin, TX 78712

Phone: 512-471-4244

E-mail: lynnkatz@mail.utexas.edu

04/15/2017

Table of Contents

1. Project Abstract

This research study is an important component of a broader comprehensive project, "Geochemistry of Interfaces: From Surfaces to Interlayers to Clusters," which sought to identify and evaluate the critical molecular phenomena at metal-oxide interfaces that control many geochemical and environmental processes. The primary goal of this research study was to better understand and predict adsorption of metal ions at mineral/water surfaces. Macroscopic data in traditional batch experiments was used to develop predictive models that characterize sorption in complex systems containing a wide range of background solution compositions. Our studies focused on systems involving alkaline earth metal (Mg^{2+}, Ca^{2+}, Sr^{2+}, Ba^{2+}) and heavy metal (Hg^{2+}, Co^{2+}, Cd^{2+}, Cu^{2+}, Zn^{2+}, Pb^{2+}) cations. The anions we selected for study included Cl^-, NO_3^-, ClO_4^-, SO_4^{2-}, CO_3^{2-} and SeO_3^{2-} and the background electrolyte cations we examined included (Na^+, K^+, Rb^+ and Cs^+) because these represent a range of ion sizes and have varying potentials for forming ion-pairs or ternary complexes with the metal ions studied.

The research led to the development of a modified titration congruency approach for estimating site densities for mineral oxides such as goethite. The CD-MUSIC version of the surface complexation modeling approach was applied to potentiometric titration data and macroscopic adsorption data for single-solute heavy metals, oxyanions, alkaline earth metals and background electrolytes over a range of pH and ionic strength. The model was capable of predicting sorption in bi-solute systems containing multiple cations, cations and oxyanions, and transition metal cations and alkaline earth metal ions. Incorporation of ternary complexes was required for modeling Pb(II)-Se(IV) and Cd(II)-Se(IV) systems. Both crystal face contributions and capacitance values were shown to be sensitive to varying specific surface area but were successfully accounted for in the modeling strategy. The insights gained from the macroscopic, spectroscopic and CD-MUSIC modeling developed in this study can be used to guide the implementation of less complex models which may be more applicable to field conditions. The findings of this research suggest that surface complexation models can be used as a predictive tool for fate and transport modeling of metal ions and oxyanions in fresh and saline systems typical of energy production waters and wastewaters.

2. Technical Report

A. Introduction

Energy production, operation and waste management practices have all contributed to environmental contamination of surface and groundwaters in the U.S. In many areas, the release of heavy metals into water and soil phases has caused aqueous concentrations of these metals to rise to unsafe levels. Remediation strategies for these pollutants require a fundamental understanding of their fate and transport in natural and engineered systems. To facilitate selection of an optimal cleanup method, fate and transport models can be utilized to ascertain contaminant mobility and to assess, in the particular background soil/water environment, the potential options for remediation. Oftentimes, the metal contaminants in question at these remediation sites are observed to adsorb to the mineral surfaces present and adsorption is often selected as the remediation technology for metal ion treatment of contaminated water.

The adsorption of transition metal cations, oxyanions and alkaline earth metal ions to aluminum, iron and silicon oxide minerals present in natural and engineered systems is highly dependent on the pH, ionic strength, and concentration of competing and co-adsorbing species in a particular system. Indeed, the

adsorption of metal cations and anions at the mineral-water interface is a complex process that may involve surface deprotonation, changes in cation solvation as the metal approaches the surface, metal hydroxylation, and metal-anion pairing. Thus, predictive models must be both accurate and comprehensive if they are to be used to guide our understanding of fate, transport and remediation.

Surface complexation models (SCMs) have shown great promise in predicting ion adsorption onto metal oxides and other variable charge surfaces. In these models, adsorption reactions are thought to be similar to aqueous complexation reactions where reactive sites present on the mineral surface act as ligands with the adsorbate. A number of different surface complexation models have been developed over the last forty years that range in complexity depending on their description of the mineral – water interface and the number of adjustable parameters required. The application of these SCMs to field scale prediction of metal ion fate and transport has evolved significantly over the last decade; however, the extensibility of these models is still hampered by several fundamental issues including mineral surface characterization, surface precipitation reactions, ternary surface complex formation, and accurate inclusion of the impacts of background solution components (background electrolytes, competing sorbates, etc.). The impact of background solution characteristics is becoming increasingly significant as water from desalination processes, fracking operations and CO_2 sequestration processes contain significant ion concentrations. This research focused on addressing several of these issues to improve surface complexation modeling of metal ion fate and transport:

1) Improved characterization of the mineral/water especially with respect to assessing adsorption site densities and characterizing the inner-layer charge distribution;
2) The potential adsorption of ternary complexes (metal-anion pairing) at oxide-water interfaces;
3) Detailed surface complexation modeling of alkaline earth metal ions over a range of background electrolytes, competing sorbates, and ionic strengths that span the range of conditions found in energy production waters.

This research was conducted as part of a larger effort led by Sandia National Laboratories entitled, "Geochemistry of interfaces: from surfaces to interlayers to clusters" Randall T. Cygan, Jeffery A. Greathouse, Louise J. Criscenti, Kevin Leung and May Nyman (Sandia National Lab); Lynn E. Katz (University of Texas at Austin); and Heather C. Allen, (Ohio State University. The comprehensive project sought to identify and evaluate the critical molecular phenomena at the metal-oxide interface that control many geochemical and environmental processes. By combining the most advanced experimental and spectroscopic methods with state-of-the-art molecular simulations, the research presents an integrated effort to improve our understanding of the mineral-water interface and to develop a predictive capability for evaluating geochemical processes that are critical to water quality and treatment, fate and transport of contaminants, radionuclide isolation and waste forms, carbon capture and sequestration, resource extraction, materials stability and corrosion, and other related technologies.

B. Background

Surface complexation theory developed from the observation that ion adsorption to mineral surfaces is analogous to the formation of solution-phase complexes [1]–[3]. In surface complexation models, adsorption of dissolved chemical species to the mineral surface is described thermodynamically via formation reactions between solutes and specific surface sites [4]. The free energies associated with these formation reactions have a chemical and electrostatic component to them, both of which are influenced by the surface sites involved [5]. A core tenet in surface complexation theory is the idea that the adsorbed ions reside at specific locations within the mineral – water interface and impact the charge at these locations. In general, there are three possible regions for ion adsorption to occur: the surface layer, the

compact layer, or the diffuse layer. These three layers comprise what is termed the electrical double layer (EDL) [5]. The charge arising from interactions between surface sites and aqueous ions is divided by Sposito [6] into two categories: net proton charge (σ_H) and net adsorbed ion charge (Δq); the latter includes inner-sphere and outer-sphere surface complexes as well as the diffuse layer of ions that provide charge balance in the bulk.

The adsorption and desorption of protons from these sites allows for a variable charge surface that is positively charged at lower pH values and becomes negatively charged as the pH of the system rises (Figure 1). Both proton adsorption and adsorption of ions as inner-sphere or outer-sphere complexes can be described by surface complexation reactions between the fixed number of surface sites and the ions. Cations that form either inner-sphere surface complexes can displace protons from the surface and anions that form inner-sphere complexes undergo ligand exchange with surface hydroxyl sites to alter the surface charge. These reactions can be described as follows:

$$\equiv SOH^0 + H^+ \leftrightarrow \equiv SOH_2^+ \qquad (K_+^{int}, \text{ protonation reaction}) \qquad (1)$$

$$\equiv SOH^0 \leftrightarrow \equiv SO^- + H^+ \qquad (K_-^{int}, \text{deprotonation reaction}) \qquad (2)$$

$$\equiv SOH^0 + Me^{2+} \leftrightarrow \equiv SOMe^+ + H^+ \qquad (K_{Me}^{int}, \text{ inner-sphere reaction}) \qquad (3)$$

$$\equiv SOH^0 + H^+ + OxAn^{2-} \leftrightarrow \equiv S(OxAn)^{1-} + H_2O \qquad (K_{OxAn}^{int}, \text{ inner-sphere reaction}) \qquad (4)$$

$$\equiv SOH^0 + Cat^{2+} \leftrightarrow \equiv SO^-\_Cat^{2+} + H+ \qquad (K_{Cat}^{int}, \text{ outer-sphere reaction}) \qquad (5)$$

$$\equiv SOH^0 + H^+ + An^- \leftrightarrow \equiv SOH^{2+}\_An^- \qquad (K_{An}^{int}, \text{ outer-sphere reaction}) \qquad (6)$$

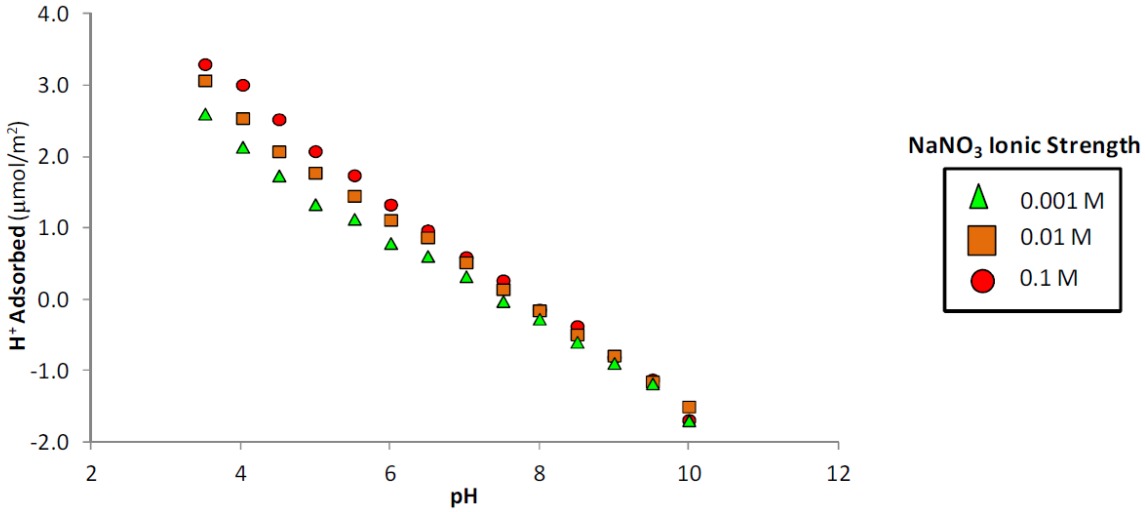

Figure 1. Potentiometric titration data for a goethite sample with a specific surface area (SSA) of 76 m^2/g using a NaNO3 background electrolyte. Data taken from Barrow and Cox [7].

In contrast to protons that are bound directly to the surface and inner- or outer- surface complexing, ions present in the diffuse ion swarm are completely dissociated from the surface and relatively free to engage in diffusive motion [5], [6].

Surface complexation models (SCMs) based on this construct follow three basic tenets associated with these reactions and electrical double layer theory [5]:

1. Adsorption/surface complexation of aqueous ions occurs at specific sites on the adsorbent's surface;
2. Surface complexation reactions can be described thermodynamically using mass law expressions that take into account the electrostatic effects of the EDL;
3. The electrostatic effects associated with adsorption (i.e., surface charge and surface potential) are accounted for in the model.

SCMs describe the surface and compact layers of the EDL as electrostatic planes termed the 0- and β-planes, respectively. These electrostatic planes run parallel to the adsorbent's surface with potentials ψ_0 and ψ_β, respectively. This theoretical construct implies that all ions adsorbed in a given layer as well as their charge, reside on the same plane and are the same horizontal distance from the mineral's surface. Therefore, although ions that adsorb in the surface or compact layers can be located on or between electrostatic planes, for modeling purposes, the charge of these adsorbed ions is placed on either the 0-plane or the β-plane. Differences among the various surface complexation models commonly used (the Diffuse Layer Model (DLM) [8]–[10], the Constant Capacitance Model (CCM) [3], [11]–[14] , various versions of the Triple Layer Model (TLM) [15]–[23], and the Charge Distribution Multi-Site Complexation (CD-MUSIC) Model [24]–[26] are in large part due to different simplifications regarding the presence of ions on particular planes, the corresponding distribution of charge, and the relationship between charge and potential in the EDL. The Diffuse Layer Model (DLM) assumes adsorption occurs on the 0-plane and the relationship between charge and potential in the diffuse layer is described by the Gouy-Chapman theory. In one triple-layer version of the surface complexation, strongly adsorbing ions adsorb on the 0-plane and weakly adsorbing ions, including the alkaline earth metal ions, adsorb onto the β -plane. This particular construct allows adsorption of strongly sorbing metal ions to be independent of ionic strength. The charge-potential relationship for these planes is assumed to be analogous to two parallel plate capacitors in series; hence, two capacitance values are required in the model. In addition, a diffuse layer is also present which is described using Gouy-Chapman theory. Various models including the Charge Distribution Multi-Site Complexation (CD-MUSIC) Model employ this construct.

Each of the common surface complexation models has been shown to describe adsorption behavior over a range of conditions; however, a number of challenges remain with respect to predicting adsorption in multi-solute systems, characterizing the reactive site density of oxide minerals, and selecting capacitance values that describe the charge/potential relationships. Finally, each model also requires selection of surface complexation reactions for protons and each metal cation or oxyanion that is consistent with crystallography, spectroscopic data and computational molecular modeling simulations.

1. Limitations in surface characterization for surface complexation modeling

As indicated previously, there are several areas in which inadequate characterization of the surface limits surface complexation modeling. Two of these areas are estimating surface site density and assigning capacitance values to the 0 and β planes. Other areas that need to be addressed include the heterogeneity of surface sites and intrinsic proton reaction constants (K_+^{int} and K_-^{int}).

Surface site density. Oxide and oxyhydroxides contain hydroxyl functional groups at the mineral surface [27]. The number of (reactive) surface hydroxyl sites present per unit surface area on a mineral surface is represented by the surface site density (N_S). Quantifying the value of Ns for particular minerals has remained a challenge for surface complexation models in part due to differences in reactivity

of different functional groups on the surface and in part because different techniques for measuring surface site density often yield different values [28]. Several different techniques such as objective curve fitting [29]–[31], crystallography [25], tritium exchange, and surface saturation data [12], [32]–[36] have been used previously to estimate the N_S parameter for adsorbents of interest. In the case of the iron (hydr)oxide goethite, N_S values determined using the methods listed above have been found to range from 0.5 to 20 sites/nm^2 [37]–[39].

In most modeling studies, once a site density value is selected for a given mineral, it is considered valid for all samples of that particular mineral. For example, the site density of 16.4 sites/nm^2, obtained from tritium exchange data for a goethite sample with a specific surface area (SSA) of 54 m^2/g, has been utilized in a number of SCM studies for goethite samples with SSAs ranging from 49 to 95 m^2/g. While this assumption regarding a uniform site density is useful in reducing the number of fitting parameters needed to run a SCM, there is strong evidence suggesting that N_S varies between mineral samples. From crystallography, it has been shown that mineral surfaces are composed of different crystal faces possessing unique site types and site densities that vary from one crystal face to another. Microscopic imaging studies have observed the contribution of these crystal faces to differ between mineral samples, especially when comparing samples with differing SSAs. Given this information, it stands to reason that the current modeling practice of using the same site density value for all samples of a given mineral is not realistic.

Although numerous modeling studies have proven successful in predicting single solute adsorption data utilizing different site densities within the range of 0.5 to 20 sites/nm^2, a number of problems have been encountered. In particular, the equilibrium constants determined for surface complexation reactions in one modeling study are not often transferrable to other modeling studies utilizing a different mineral sample or employing a different site density value. This result has poor implications for field scale predictions where constants generated from one site are unlikely to be extensible to other field sites. Furthermore, SCM predictions of ion adsorption in multi solute systems are often inaccurate; a result that is believed to be due, at least in part, to the site density value(s) employed in the model. In summary, different techniques have been utilized by researchers to estimate Ns for adsorbents of interest. In the case of goethite, the N_S values determined with these methods ranges from 0.5 to 20 sites/nm^2. Typically, a single site density value is employed for all samples of a given mineral or the N_S value predicted from a particular technique is used to estimate a mineral's site density [28]. Both of these approaches disregard all other N_S values that were predicted from theoretical and experimental studies of goethite. Hence, there is a need for a methodology to be developed that unifies the different site density values predicted and explain their apparent incongruence.

Capacitance values. Capacitance values of an electric double layer at a mineral-water interface are not directly measured; values are commonly considered an adjustable fitting parameter and determined by optimizing their values to fit potentiometric titration data sets [37], [40]. Titration data relate the surface charge value (σ_0) with the solution pH [24], [41]. However, capacitance values are theoretically related to the distance of approach of the ions to the surface, which means that the range of possible values of capacitance is constrained by solution chemistry and dimensions of the interfacial region [42]–[44]. Since capacitance values need to be physically realistic, it has been suggested that the optimized values should be somewhat independent of a particular surface complexation model [39], [42], [45]. The theoretical relationship between capacitance value and distance of approach of ions is: $C = \varepsilon_0 \varepsilon_r / d$, where ε_0 and ε_r are the absolute (8.85 X 10^{-12} CV^{-1}m^{-1}) and relative dielectric constant, respectively [43].

As indicated, many surface complexation constructs employ an inner and outer layer for adsorption which constrain the location of ion complexes relative to surface ligands [46]. The two layers may act as

separate parallel plate capacitors, thus having two different capacitance values: C_1 and C_2. For proton adsorption, however, the effect of C_2 is known to be minimal in simulating potentiometric titration data, while C_1 directly impacts the surface charge calculation [23]. Thus, finding a value of C_1 is commonly regarded to be one of the main objectives in fitting surface charge data. In early studies, the C_2 value was commonly assumed to be a fixed value of 0.2 F/m^2 in the triple layer model (TLM), based on direct measurements of the AgI-electrolyte interface [37], [47]. However, more recent studies have pointed out that the assumption that AgI could be used as a surrogate for oxide minerals was based on a misinterpretation of the relationship between the double layer properties of AgI and that of metal (hydr)oxides [24], [41], [43], [44]. Thus, modeling studies now often use the approximation that C_2 is equal to C_1 [48]–[51]; Hiemstra and Van Riemsdijk (2006) [44] and Sverjensky (2005) [23] were able to accurately simulate proton adsorption using this assumption.

It has also been suggested that the capacitance is related to the surface roughness of minerals such as goethites [45] and that goethites with lower specific surface area (SSA) tend to have greater surface roughness compared to higher SSA goethites [52], [53]. The basis for this hypothesis is that adsorbed protons may locate closer to rough surfaces compared to smooth surfaces. Thus, for a rough surface, the inner and outer layers of the EDL would be thinner which leads to higher capacitance values [45], [54].

2. Selection of surface complexes

Over the past several decades significant progress has been made in improving surface complexation modeling through more accurate selection of the operative surface complexes. The selection of inner-sphere, outer-sphere, mono-dentate, bi-dentate or multi-dentate complexes has grown tremendously since the early work of Hayes and co-workers who employed x-ray adsorption spectroscopy to identify inner-sphere sorption of selenite and outer-sphere sorption of selenite on goethite and incorporate those complexes into their surface complexation modeling [55]. The use of in-situ techniques such as x-ray absorption spectroscopy (XAS), FTIR and X-ray standing wave spectroscopy (XSW) have enabled modelers to constrain the number of surface complexes considered during modeling. These approaches have been instrumental in modeling single-solute systems. Molecular modeling approaches have also helped constrain the selection of surface complexes in single solute systems.

While numerous modeling studies predicting ion adsorption in single solute systems has been successful [e.g. [7], [41], [48], [51], [56]–[62]], fewer studies have attempted to model more complex systems possessing multiple anion adsorbates [48], [53], [63], cation adsorbates, or a combination of both [64]–[67]. Modeling adsorption in these more complex, multi-solute environments, has proven difficult because the model must be able to take into account site competition and electrostatic effects that are caused by the presence of multiple adsorbates in the system [41], [68]–[70]. Successful prediction of adsorption in these multi-solute systems has required the use of surface species not supported by spectroscopic evidence and/or adjustment of other model parameters such as the specific surface area (SSA) of the mineral sample [48], [58], [63], [67], [71].

Of particular interest is the more recent spectroscopic work identifying ternary complexes such as Pb(II)-chloro [72], Pb(II)-carbonate[73], Pb-sulfate [74] Hg-Cl [75] and Cd(II)-orthophosphate [76] that suggest ternary complex formation on oxide surfaces. These data suggest that spectroscopic guidance can be used to provide guidance for modeling sorption in more complex multi-solute systems.

3. A closer look at alkaline earth metal ion adsorption

Alkaline earth metals are abundant in natural and engineered waters, and often times are present in high concentrations relative to regulated contaminants of concern [64], [69], [77]–[83]. While the importance

of understanding the fate and transport of alkaline earth metals is often overlooked, their presence at high concentrations can have significant impacts on the fate of toxic metal ions, oxyanions, radionuclides and even organic contaminants [22], [64], [69], [79], [80], [84]. In particular, extremely high concentrations of these metals (e.g. 3,000 – 30,000 mg/L of Ca) are commonly found in ground waters, produced waters, recycled fracking waters, and wastewaters from soil remediation sites [69], [77]–[83]. While alkaline earth metals such as Mg and Ca are generally considered to be weakly adsorbed to common soil minerals such as iron oxides, accurate modeling of their adsorption is required for predicting the adsorption of other weakly and strongly adsorbing solutes [22], [64], [69], [79], [80], [84].

Although there have been numerous studies which elucidate the adsorption behavior of alkaline earth metals, there is still a lack of agreement on many adsorption characteristics of these metals including, but not limited to, the mode of adsorption (inner- or outer-sphere), complex structure (monodentate, bidentate or tetradentate complexes) and surface affinity [22], [64], [85]–[103]. This has been partially due to the lack of molecular modeling and/or spectroscopic data identifying the structure of surface complexes for the dominant alkaline earth metal ions (e.g. Ca^{2+} and Mg^{2+}). Another reason for the insufficient understanding of alkaline earth metal adsorption is presumably due to the common assumption of inert or indifferent background electrolytes [22], [69]. Most experimental studies have conducted experiments using simple monovalent electrolyte systems, such as NaCl, $NaNO_3$, $NaClO_4$ and KNO_3. However, recent studies have started to investigate potential impacts of the interaction between the background electrolytes, sorbed ions and surfaces at the water-mineral interface. As an example, recent molecular modeling studies have suggested that alkali metal ions such as Na^+ form inner-sphere surface complexes which suggests that their impact on strongly sorbing transition metal ions may be more significant than originally thought (Unpublished study by Criscenti et al.). Hence, investigation on adsorption in various electrolyte systems is critical for the isolation of these electrolyte effects and for identifying the true adsorption behavior of alkaline earth metals independent of the particular background electrolytes in the system. Moreover, prediction of ion adsorption in saline systems typical of produced waters, desalination waters and other energy waste streams requires incorporation of these species into surface complexation models.

C. Experimental and Modeling Approach

1. Experimental Systems

A number of different mineral oxides were used in this research including silica, ferrihydrite, goethite and gibbsite. The preparation and characterization of these materials varied depending on the research focus at the time.

Silica. The crystalline silica used was Min-U-Sil® 5 obtained from U.S. Silica (Berkeley Springs, WV) with 96.3% finer than 5 microns and a median diameter of 1.6 microns. The silica was prepared with a procedure modeled after MacNaughton and James [104] by first firing in a furnace at 550°C for 24 hours to remove volatile contaminants. Following the furnace, the silica was boiled in 4N ACS-grade hydrochloric acid (HCl) for 4 hours, and then rinsed with CO_2 free Milli-Q water repeatedly until the pH of supernatant reached neutral and the conductivity was less than or equal to 20 microsiemens per centimeter. After rinsing, the silica was stored in a slurry form with the same background electrolyte used in the adsorption experiments in a nitrogen-purged glove box until needed.

The crystal structure of Min-U-Sil® 5 was confirmed to be α-quartz using powder x-ray diffraction (XRD, Siemens D500). The BET surface area of the silica was determined to be 4.00 ± 0.02 m^2/g using nitrogen gas adsorption (Quantachrome, Autosorb-1).Fumed silica (from Sigma, St. Louis, MO) was used as the substrate for Co(II) and Sr(II) XAS experiments and macroscopic sorption experiments due to its

high surface area relative to Min-U-Sil® 5 which was also used to study sorption mechanisms of Pb(II), Co(II) and Sr(II). The fumed silica was used as received without further treatment except for rinsing several times with Milli-Q treated water followed by a 0.01 M $NaNO_3$ solution. A stock solution of the fumed silica was prepared at a solid concentration of 15 g/L in a 0.01 M $NaNO_3$ solution 48 hours prior to preparation of the experimental samples to insure full hydrolysis of the solid surfaces.

Gibbsite. The adsorbent, OC-1000 gibbsite ($Al(OH)_3$) was obtained from Almatis (Bauxite, AR) with a surface area of 2.19 m^2/g. The point of zero salt effect (PZSE) of the adsorbent of 9.8 was determined by potentiometric titration method. The solid was used as obtained without further purification. The solid was hydrated with 0.001M $NaNO_3$ at a concentration of 100 g/L in a glove box with N_2 for at least 48 hours before used in experiments.

Ferrihydrite. Methods for preparing ferrihydrite have been well documented [105], [106]. Ferrihydrite was precipitated from the rapid titration of a 0.33 M reagent grade ferric nitrate [$Fe(NO_3)_3 \cdot 9H2O$] (EM Science, Gibbstown, NJ) solution to pH 7 using 1N sodium hydroxide (NaOH) according to a previously developed method [105]. Inside a nitrogen-purged glove box, 40 g of ferric nitrate [$Fe(NO_3)_3 \cdot 9H_2O$] were added to 300 mL of CO_2 free water in a 1000 mL Teflon beaker with a magnetic stirring bar placed at the bottom to provide mixing. Preparation of the 1N NaOH utilized 450 mL of CO_2 free H_2O that was mixed with 50mL of 10N NaOH (Dilut-it). The pH-meter (Orion 920A) was calibrated using 3 standards with pH = 4, 7, and 10. Next, the 0.33N ferric nitrate solution was titrated with 1N sodium hydroxide to pH 7. Then, the solid precipitated slurry was placed in centrifuge bottles and washed. This step was completed within 24 hours to avoid aging effects. The presence of 2-line ferrihydrite was confirmed using x-ray diffraction and a pH_{pzc} of 8 was determined.

Goethite. Goethite was prepared according to the method described by Schwertmann et al. [107], Peak et al. [108] and further refined by Vieira [109], where $Fe(NO_3)_3$ was used as the precursor and aged for 14 days in KOH solution at 25°C. The entire synthesis process was performed inside a N_2 gas-filled glove box (Protector®, Labconco, Kansas City, MO) in order to minimize potential contamination of CO_2, and degassed CO_2-free ultrapure water of 18.2MΩ-cm resistivity (Barnstead™ Nanopure™, Thermo Fisher Scientific, Waltham, MA) was used to wash out impurities left on the solids. Characterization of solids were done by N_2-BET (Quantachrome Instruments, Boynton Beach, FL) and XRD (Philips Analytical, Amsterdam, Netherlands), and pH_{pzse} of goethite was determined by potentiometric titration [4]. Three different types of goethite were prepared, each having specific surface area (SSA) of 50, 64.5, and 73 m^2/g, respectively. The SSA value of goethite were similar to values reported in previous studies using the same preparation method [109], [110]. The pH_{pzse} = 9.1 was also within the range of 9.0 – 9.5 which is documented by many studies [39], [45], [52], [111], [112].

2. Potentiometric Titrations

Titration experimental results are often used to estimate several parameters required in surface complexation models including the acidic constants (K^-_{int} and K^+_{int}), the background electrolyte equilibrium constants (K_{cat}^{int} and K_{an}^{int}), and one of the capacitance terms (C_1). Additionally, titration data are used to determine the pH of the point of zero salt effect pH_{PZSE}, which is an estimate of the pH of the point of zero charge (pH_{PZC}) of the adsorbent.

To this end, potentiometric titrations of the adsorbents were performed in a 400-mL Teflon beaker kept in a controlled temperature room at 25 ± 0.5 °C. In order to prevent carbon dioxide (CO_2) from entering the system, an inert N_2 atmosphere was maintained by purging the system with high purity N_2 gas. Reagent grade nitrate salts were added to the known solids concentration slurry to achieve the desired ionic strength value. Then, the titration was conducted in an automatic titrimeter by sequential base addition

and pH measurement. At the end of the titration, sequential acid additions and pH measurements were made as the pH was lowered, and finally base was added again to raise the pH back to the starting value. Titrations were performed on each adsorbent at three different ionic strengths, to obtain a set of titration curves.

3. Batch adsorption experiments

Batch adsorption experiments were conducted throughout this research with different mineral oxides, involving alkaline earth metal (Mg^{2+}, Ca^{2+}, Sr^{2+}, Ba^{2+}) and heavy metal (Hg^{2+}, Co^{2+}, Cd^{2+}, Cu^{2+}, Zn^{2+}, Pb^{2+}) cations. The anions we selected for study included Cl^-, NO_3^-, ClO_4^-, SO_4^{2-}, CO_3^{2-} and SeO_3^{2-} and the background electrolyte cations we examined included (Na^+, K^+, Rb^+ and Cs^+). In most cases, stock solutions containing adsorbent media particles, alkaline earth metal ions and background electrolyte reagents were prepared from degassed CO_2-free ultrapure water and high purity salts (> 99.999%, Puratronic® by Alfa Aesar or equivalent). Metal ion stock solutions were acidified to 0.318 N nitric acid (Trace metal grade, Fisher Scientific) for preservation. The electrolyte stock solutions were made from high purity $NaNO_3$, NaCl, $NaClO_4$, KNO_3, $RbNO_3$, and $CsNO_3$ salts at multiple concentrations ranging from 0.01 M to 0.7 M. The whole process of preparing the stock solutions and batch reactors was preformed inside an N_2 gas-filled glovebox to avoid introduction of carbonates.

The basic procedure for conducting the batch experiments involved adding the specified quantities of stock solutions to 15 mL polypropylene vials. Once the contents of the batch reactors were added, pH was adjusted using either 0.1N HNO_3, 0.1N HCl, 0.1N $HClO_4$ or 0.1N NaOH depending on the electrolyte composition and target pH. Reactors were then placed on a shaker in a 25°C temperature controlled room for equilibration. Equilibration time was set to 24 hours, based on expected times to equilibrium [24], [42], [95], [113], [114]. After equilibration, samples were taken out of the reactors and either centrifuged and/or filtered with 0.45 μm Polyethersulfone (PES) membranes for analysis.

The metal cation composition of each filtered sample was analyzed by inductively coupled plasma - optical emission spectrometry (ICP-OES) (ICP 710, Agilent Technologies, Santa Clara, CA) or graphite furnace atomic absorption spectroscopy (Perkin-Elmer) depending on the concentration range and analyte. The pH of each reactor was measured in a N_2-filled glovebox at 25°C, with a Thermo Orion® ROSS® combination pH electrode (8103BNUWP).

4. Surface Complexation Modeling

A number of surface complexation models were employed in this research including the diffuse layer model (DLM) for modeling single and bi-solute Cu(II), Pb(II) and Cd(II) sorption onto ferrihydrite [115] , triple layer modeling of Cd(II), Pb(II) and Se(IV) single and bi-solute data onto ferrihydrite and goethite [109] . Upon completion of that early effort, it became clear that neither of these models could adequately capture adsorption over the range of behavior expected in the field, even though both modeling efforts were based on surface complexes determined from x-ray absorption spectroscopy and significant efforts were made to account for potential precipitate formation, aqueous complexation and surface polymerization. As a result, in the final years of the project modeling efforts focused on the CD-MUSIC model and relied heavily on modeling goethite as a model sorbent.

The CD-MUSIC surface complexation model was used in this study to describe and predict surface reactions. The CD-MUSIC model incorporates the MUSIC surface complexation model with a charge distribution model [24]. It describes the mineral-water interface with three electrostatic planes (the 0-, 1-, and d-plane) as in the case of the TLM. The MUSIC model utilizes crystallographic information to describe protonation and reactive site densities of specific surface sites of adsorbent minerals [24], [40].

Three different oxygen-terminated groups at the goethite surface are identified in the MUSIC model; which are oxygen groups that are singly, doubly, and triply coordinated to the central Fe atoms. These surface sites have distinctive surface charge, proton affinity, reactivity, and densities. The capability to account for surface heterogeneity through crystal face distributions is one of the advantages of the MUSIC model [24], [26], [45], [116], [117].

The CD model accounts for the physical size of sorbed ions instead of assuming that they are point charges like many other SCMs [24]. This means that the charge of the ions does not need to be located on a specific electrostatic plane but can be distributed over multiple planes. This interpretation of surface complexation is incorporated into the electrostatic calculations through the apportioning of the ionic charge to different planes [24], [42], [113]. The charge from protonation or deprotonation are all attributed to the 0-plane, while the charge from inner-sphere complexes are distributed between 0- and 1-planes. The charge distribution of inner-sphere complexes is determined by the number of ligands shared with the surface and the bond strength [113]. For outer-sphere complexes and ion pairs, the charges were originally located on the d-plane which designates the head end of the diffuse layer [40], [41]. However, a study by Rahnemaie et al. (2006) [42] revealed that there is charge separation between the minimum distance of approach of the ion-pairs and the head end of the diffuse layer. Due to this finding, current SCM studies which utilize CD-MUSIC places charge for outer-sphere complexes and ion-pairs on the 1-plane [44], [48]–[51], [66], [118].

The charge distribution values and equilibrium constants of the ion-pair reactions between background electrolyte and surface sites can also be defined. Monovalent ions, such as Na^+ and NO_3^-, are normally assumed to be adsorbed as outer-sphere monodentate complexes on oxide surfaces [15], [42], [86], [113], [119], [120]. Hence, the charge distribution of Na^+ and NO_3^- on the 0-plane and β-plane are set to $\Delta z_0 = 0$, $\Delta z_1 = +1$ and $\Delta z_0 = 0$, $\Delta z_1 = -1$, respectively in this study.

Reaction constants and surface parameters for the CD-MUSIC model were determined through fitting experimental potentiometric titration data and adsorption data using the computer software packages FITEQLC [121] and FITEQL 4.0 [122]. Parameter estimation was typically performed in several distinct steps: (1) simulation of the potentiometric titration data for the goethite surface to determine the intrinsic surface protonation and ion pair formation equilibrium constants; (2) fitting the single solute pH adsorption edge experimental data conducted on the goethite to obtain the equilibrium constants for each ion's surface complexes; (3) simulating the single solute isotherm adsorption experiments and the bi-solute adsorption edge experiments conducted utilizing the same parameters, surface species, and affinity constants previously determined in steps 1 and 2. In summary, the potentiometric titration data and single solute pH adsorption edge data were used for each ion to calibrate the CD-MUSIC model. The single solute isotherm data and bi-solute adsorption edge data were used to substantiate the model's predictive capability. Model predictions were also conducted over varying ionic strengths. Aqueous metal speciation was calculated in FITEQLC [121] using the equilibrium constants supplied in Visual MINTEQ at 25°C. The model's performance in predicting adsorption edge and isotherm data was quantified for each data set by calculating the weighted sum of squares divided by degrees of freedom (WSOS/DF). WSOS/DF values between 0.1 and 20 are considered to be satisfactory model fits of the experimental data [122].

In order to model adsorption, the surface complex species must be properly determined. The structure and location of surface species are commonly identified by conducting molecular modeling [95], [98], [100] and spectroscopic analysis [41], [55], [93], [123]–[125]. Spectroscopic data and computational molecular modeling simulations found in the literature were used to guide the selection of surface complexes employed in the CD-MUSIC model. Bond valence analysis as described by Bargar et al. [72], was also be used to help elucidate the identity of each surface species used in the model. For example,

many studies examining Sr^{2+} have identified the surface complex species on goethite using various methods [22], [64], [85], [86], [91]–[94]. Although there is a lack of agreement on what the actual structures are for Sr-goethite complexes, most researchers agree that they exist as outer-sphere complexes. In addition, many studies have suggested tetradentate surface complex species with the rutile surface [97]–[100]. Therefore, these findings served as the starting point for selecting the surface species which most accurately fit experimental data.

Finally, one of the goals of this research was to determine a strategic approach for estimating surface site density and capacitance as a function of the surface area of goethite. Potentiometric titration data, maximum oxyanion adsorption data, crystallography and tritium data were used to develop an approach that reconciles the different values of surface site density often obtained from these data. The approach builds on previous research by Villalobos and co-workers [60] termed the crystal face composition (CFC) approach. Potentiometric titration data was also analyzed for goethites having different surface areas (different CFCs) to determine a relationship between surface area and capacitance value.

D. Results and Discussion

1. Macroscopic Adsorption Behavior

Silica. Initial research in this project sought to identify systems in which ion-pair (e.g. Pb-Cl, Co-Cl, Co-NO_3) surface complexes were evident. Macroscopic sorption data was combined with aqueous speciation calculations and x-ray absorption experiments to assess whether ion-pair sorption complexes were possible. Metal sorption mechanisms were investigated for strontium, cobalt, and lead using sodium chloride, sodium nitrate, and sodium perchlorate as background electrolytes and quartz as the adsorbent. Spectroscopic analyses of concentrated sorption samples were evaluated for their ability to provide insight into the controlling sorption process for more dilute systems. For strontium, outer-sphere complexes identified using x-ray absorption spectroscopy (XAS) of concentrated samples were consistent with macroscopic sorption data collected in more dilute systems. XAS results indicated that cobalt formed a new solid phase upon sorption to silica. Macroscopic experiments and solubility modeling (Figure 2) of cobalt sorption supported the spectroscopic data for total cobalt concentrations of 10^{-5} M regardless of the background electrolyte composition or concentration. While other researchers have attributed an ionic strength of Ni(II) adsorption to Ni-ClO_4 ternary complexes, no evidence for such complexes were identified in this research [126]. At a lower total cobalt concentration (10^{-6} M), adsorption appeared to be the prevailing mechanism of cobalt removal. Spectroscopic results suggested that lead adsorbed as an inner-sphere complex on silica. The decrease of lead removal with increasing chloride concentration was attributed to competition with aqueous lead-chloride complexes based on thermodynamic calculations. These results are reported in Chen et al. (2006) [96].

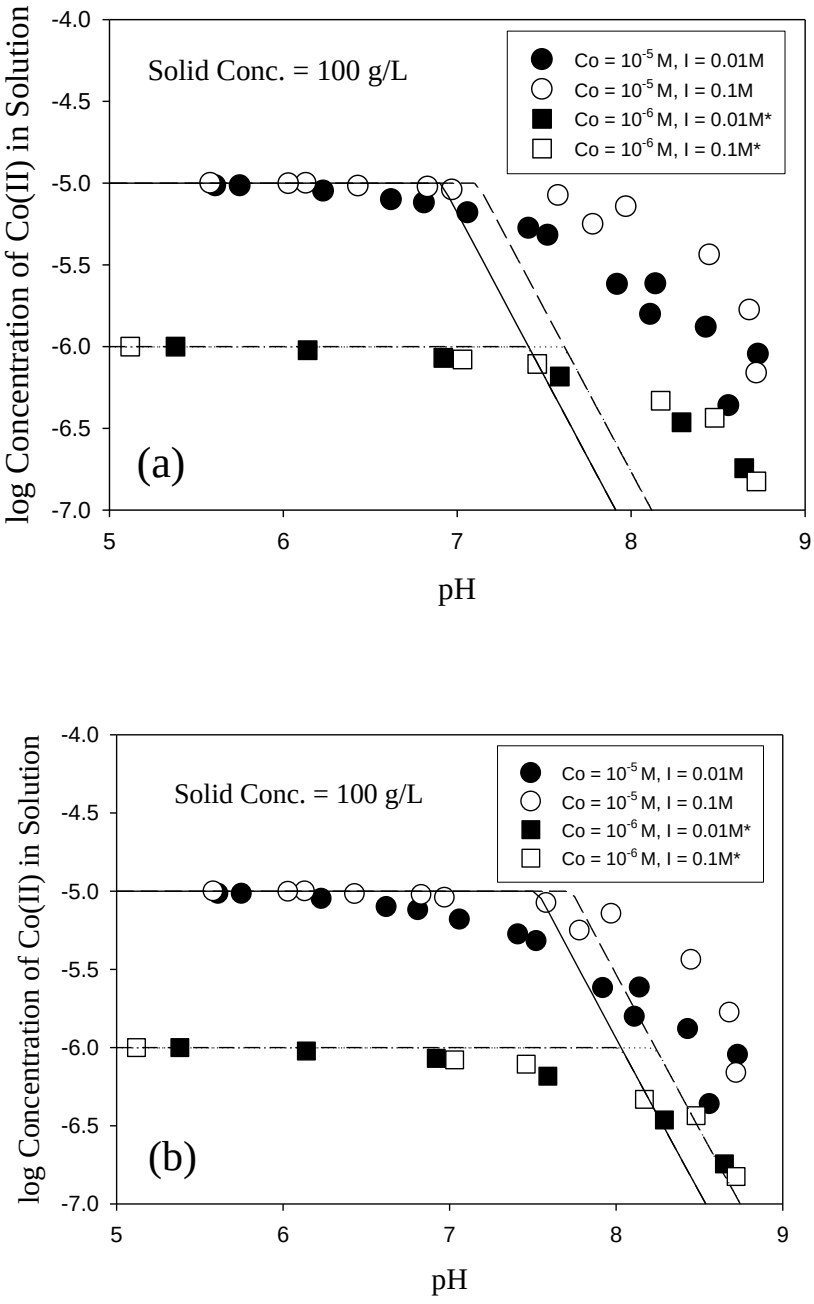

Figure 2. Comparison of aqueous Co(II) data from sorption experiments to aqueous concentrations predicted based on Co-kerolite solubility. Co(II) adsorption data are for $NaNO_3$ background electrolyte concentrations of 0.01M and 0.1 M. Co-kerolite solubility is calculated based on the range in the equilibrium constant (K_{so}= $10^{-15.1}$ for 5a and K_{so} = $10^{-18.8}$ for 5b) reported by Manceau et al. (1999) [127], and Si concentrations measured from the sorption experiments. The solid and dashed lines represent aqueous cobalt in solution for a total initial cobalt concentration of 10^{-5} M at ionic strength (I.S.) of 0.01 M and 0.1 M, respectively. The dash-dot and dotted lines represent aqueous cobalt in solution for a total cobalt concentration of 10^{-6} M at an I.S. of 0.01 M and 0.1 M, respectively.

Gibbsite. Two approaches, macroscopic adsorption experiments and molecular dynamics simulations, were employed to study the effect of temperature on alkaline earth metal ion adsorption to gibbsite surfaces. Increased reaction temperature enhanced the extent of metal ion adsorption for all of the alkaline earth metals studied. Whereas Mg^{2+} and Sr^{2+} (Figure 3) adsorption displayed dependence on ionic strength with increasing temperature, Ba^{2+} adsorption (Figure 4) exhibited less dependence on background ionic strength regardless of temperature. The ionic strength dependence was attributed to outer-sphere complexation and triple layer surface complexation modeling supported these results. Results from molecular dynamics simulations were in agreement with changes from outer-sphere to inner sphere complexation as a function of temperature and with periodic trends. The amount of thermal energy required to remove waters of hydration from the metal cation and the ratio of outer-sphere to inner-sphere complexation decreased with increasing ionic radii.

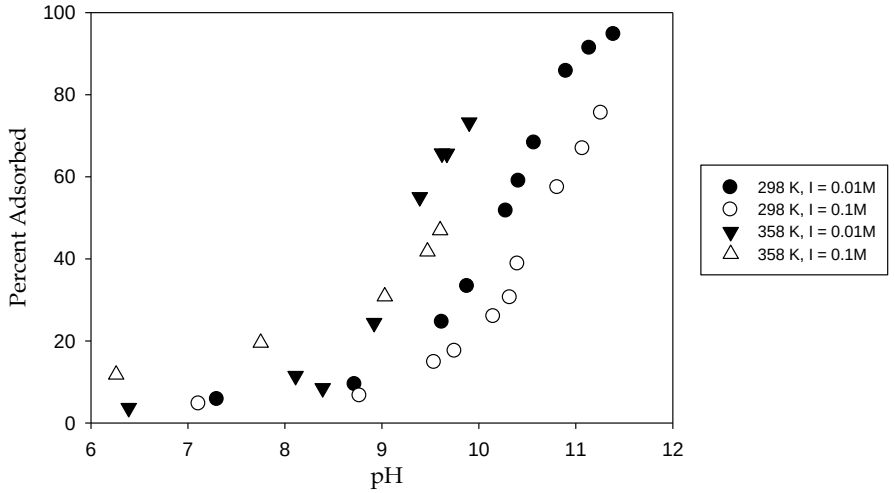

Figure 3. Sr^{2+} (Sr_{Total} = 2 x 10^{-7} M) adsorption isotherms on gibbsite (10 g/L) at 298 K and 358 K with $NaNO_3$ as background electrolyte.

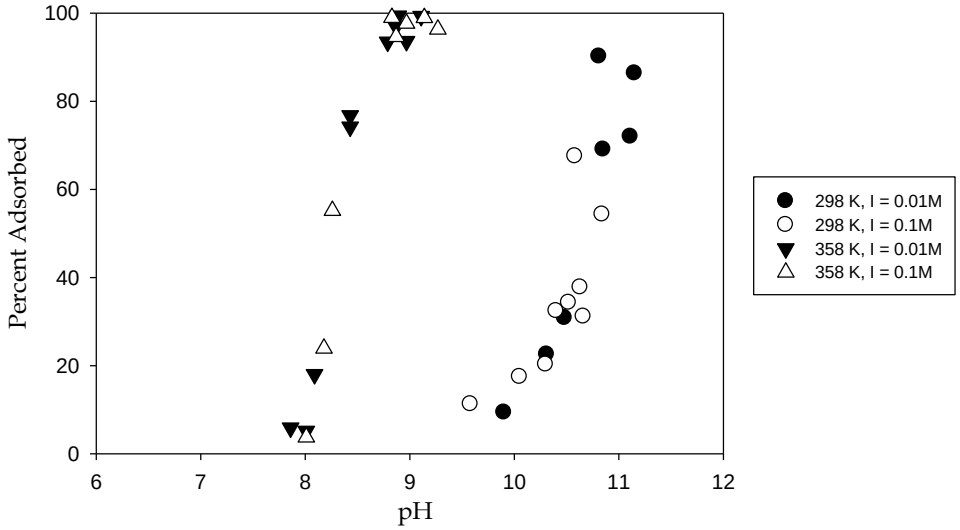

Figure 4. Ba^{2+} (Ba_{Total} = 1 x 10^{-6} M) adsorption isotherms on gibbsite (10 g/L) at 298 K and 358 K with $NaNO_3$ as background electrolyte.

Goethite. A significant effort was put forth in the collection of extensive adsorption data of alkaline earth metal ions (Mg^{2+}, Ca^{2+}, Sr^{2+}, and Ba^{2+}) on goethite over a range of ionic strengths, background electrolyte anions and background electrolyte cations. There have been few studies that extensively examined the effects of such complex matrices of solution chemistry on the adsorption behavior of alkaline earth metals. The adsorption batch test results that were collected in this study displayed several important adsorption trends which may aid in characterizing the structure and location of alkaline earth metal surface complexes within the interfacial region, which are currently less understood and controversial compared to transition metals.

One significant trend that was found from our test results was that the impact of ionic strength on metal cation adsorption on goethite increases proportionally with the crystal radii of the cations, which follows: $Mg^{2+} < Ca^{2+} < Sr^{2+} < Ba^{2+}$. Figure 5 shows the adsorption edges of the four alkaline earth metals on goethite in various ionic strength solutions. It can be clearly seen that the separation of adsorption curves among different ionic strength is smallest for Mg^{2+} and largest for Ba^{2+}. This trend differs from that observed in our previous work with gibbsite.

Another trend that was observed from this study was the inverse correlation between the crystal radii of alkaline earth metals and their affinity for goethite (Figure 5). This trend is identical with the trend seen with gibbsite in our previous study, and with predictions made by Sverjensky (2006) [22]. The results indicate that smaller cations tend to adsorb more strongly to goethite and gibbsite despite their larger hydration energies, due to low dielectric constants of the solids.

The impact of background electrolyte cation also demonstrates differences between Ba^{2+} and Mg^{2+} adsorption (Figure 6). At the same ionic strength, Na^{+} leads to reduction in Ba^{2+} sorption, whereas no impact is observed for Mg^{2+}. The observed trend for $Ba^{2+}$is consistent with increased adsorption for larger electrolyte cation radii.

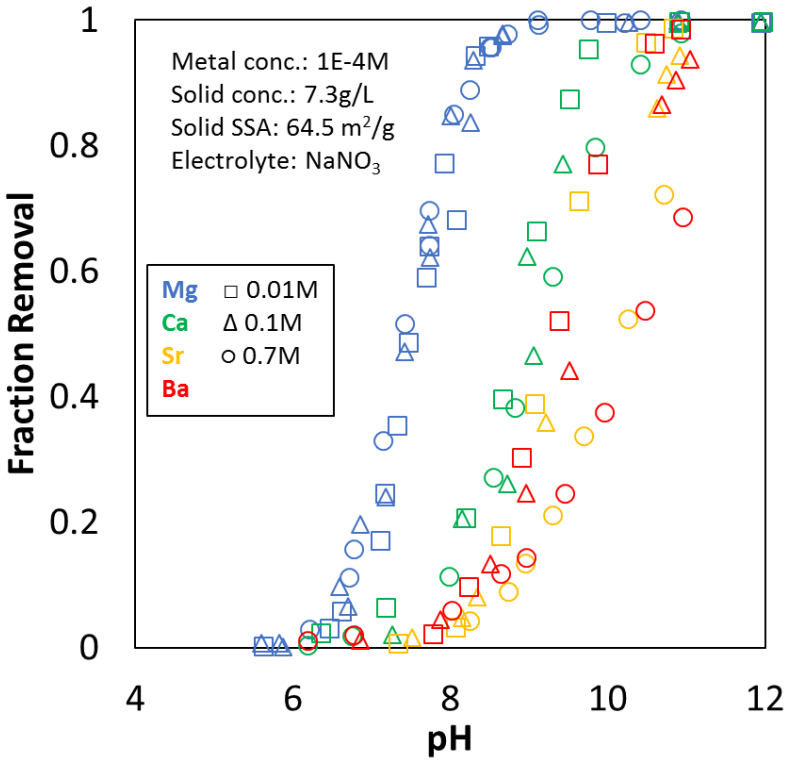

Figure 5. Impact of electrolyte concentration ($NaNO_3$) on alkaline earth metal ion adsorption.

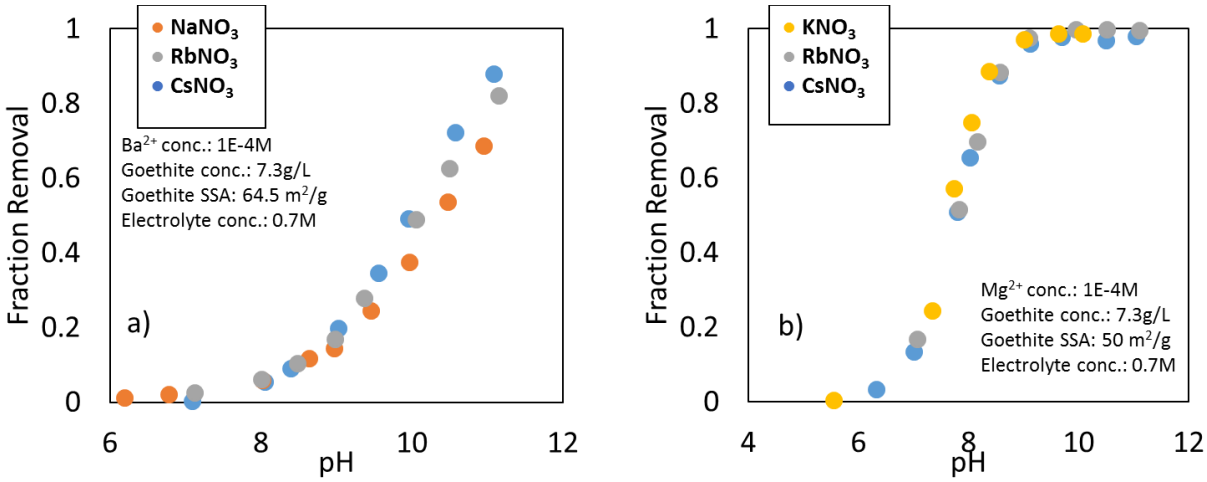

Figure 6. Impact of electrolyte cations on alkaline earth metal ion adsorption to goethite.

The impact of electrolyte anions also showed a greater impact on Ba^{2+} compared to Mg^{2+}. However, this was in part attributable to aqueous speciation modeling which showed that $BaNO_3$ complexes were significant. Thus, the amount of free Ba^{2+} in solution was lower than Mg^{2+}.

The results from the macroscopic adsorption experiments highlight the importance of considering background electrolytes in solution for adsorption of alkaline earth metals; at least two different mechanisms are operative. First, the effect of the electrolyte will depend on the relative affinity of the cations to the surface due to competition. Another important factor related to electrolyte effects is the formation of aqueous complexation of alkaline earth metals with anionic electrolytes. It was shown in

this study that altering the anionic electrolyte affects the adsorption of alkaline earth metals by changing the fraction of free metal ions in solutions. In other words, less availability of free metal ions results in less total adsorption to the surface. Regardless of the mechanisms attributing to the impact of background electrolytes on alkaline earth adsorption, the concentration of electrolyte plays an imperative role. Generally, background electrolytes have weak complexing power which is why they are commonly considered inert in many adsorption studies. However, high concentrations of these electrolytes can compensate for their weak reactivity, and their effect on metal adsorption may be significant especially in saline solutions.

2. Goethite Site Density Estimation

Mineral surfaces are comprised of crystal faces that are specific to a given mineral [53], [128]–[130]. These crystal faces possess surface functional groups (i.e. adsorption sites) that can vary in type and density (sites/nm^2) from one crystal face to another. Each type of surface functional group, herein referred to as surface site type, is thought to possess its own unique reactivity to adsorbing ions, including protons [41], [46], [118], [131]. Furthermore, adsorption studies utilizing spectroscopy, computational molecular modeling, bond valence analysis or some combination thereof, have revealed that site reactivity varies depending on the adsorbate, the surface site type, and the coordination environment [41], [48], [66], [72], [73], [75], [118], [132]–[139]. Since the surface site type, site density, and coordination environment can vary depending on the crystal face considered, the mineral surface's morphology or crystal face composition (CFC), greatly affects its reactivity [25], [26], [53], [60], [140].

In the case of the iron hydroxide mineral goethite, researchers have typically assumed the mineral surface to be composed of 90% (101) face and 10% (210) face, regardless of mineral sample in question [41], [42], [48], [50], [63], [67], [86]. While this approach for estimating CFC provides a simple and straightforward method for determining the N_S of each surface site type considered, it fails to account for the differences in reactivity and CFC that have been observed for goethite both experimentally and through microscopic image analysis [24], [25], [28], [39], [45], [52], [60], [61], [116], [140]. As a result, in order to attain satisfactory model fits using the 90% (101) and 10% (210) CFC, researchers have needed to adjust the SSA of goethite samples or utilize surface species not consistent with spectroscopic observations [48], [63], [67].

Goethite is comprised of singly, doubly, and triply coordinated sites. Mounting evidence suggests that doubly coordinated sites on goethite are nonreactive to protons at environmentally relevant pHs; however, singly and triply coordinated surface oxygens are considered to be proton reactive, with log K_H's of ≈ 8 and 11.7, respectively [41], [46], [53], [66], [131], [140], [141]. The (101) and the (001) crystal faces of goethite both possess singly, doubly, and triply coordinated surface sites (cf. Table 1) [116]. All singly and doubly coordinated sites present on these two crystal faces have a surface oxygen atom with a low proton affinity (OII). In addition, one third of the triply coordinated sites found on the (101) and (001) faces also possess

Table 1. Site types and site densities (sites/nm2) present on the predominant crystal faces of goethite.

Surface Site Type	Crystal Face N_s (sites/nm^2)			
	(101)[a]	(001)[b]	(210)[a]	(010)[c]
$\equiv FeO_I$	0	0	3.75	9.1
$\equiv FeO_{II}$	3.03	3.34	3.75	
$\equiv Fe_2O_I$	0	0	3.75	9.1
$\equiv Fe_2O_{II}$	3.03	3.34	3.75	
$\equiv Fe_3O_I$	6.06	6.68	0	0
$\equiv Fe_3O_{II}$	3.03	3.34	0	0

Site densities are taken from: a) Venema et al.[131], b) Gaboriaud and Ehrhardt [116], and c) Lutzenkirchen et al. [28]

an O_{II} surface oxygen; the other two thirds are comprised of a surface oxygen with a high proton affinity (O_I) [41], [46], [116], [131]. The combination of two triply coordinated sites, one with high and the other with low proton affinity ($\equiv Fe_3O_I$ and $\equiv Fe_3O_{II}$, respectively), has been found to render both surface sites inert [25]. For this reason, only one third of the triply coordinated sites present on the (101) and (001) crystal faces are considered reactive. On the (210) and (010) capping/terminal faces of goethite, only singly and doubly coordinated sites are present, and in the case of the (210) face both surface groups are comprised of equal amounts of low and high proton affinity oxygens [131]. To our knowledge, the distribution of sites with low and high proton affinity oxygens on the (010) face has not been determined.

Once a CFC is established for a given mineral sample, the different site types and their respective site density values can be determined for goethite using the crystallographic information presented in Table 1. Previous modeling studies that have estimated the CFC of goethite have typically considered only two crystal faces to be present on the mineral surface, either the (101) and (210) [41], [48], [51], [58], [67], the (101) and (001) [116], or the (101) and (010) [53], [60]; resulting in a total of eight, eight, and six possible site types, respectively. To make the SCM more manageable, certain assumptions regarding the site types present on the different crystal faces are employed. In particular, doubly coordinated sites on the (101) and (001) crystal faces are not considered reactive [41], [46], [53], [116], [118], the combination of one $\equiv Fe_3O_I$ site and one $\equiv Fe_3O_{II}$ site is thought to result in both sites being unreactive [25], $\equiv FeO_I$ and $\equiv FeO_{II}$ sites on the (210) and (010) crystal faces are equivalent [41], [53], [60], [67], and $\equiv Fe_2O_I$ and $\equiv Fe_2O_{II}$ sites on the (210) and (010) crystal faces are equivalent. These assumptions result in a simplified description of the interface (Table 2).

Table 2. Simplified site types and site densities (sites/nm^2) present on the predominant crystal faces of goethite.

Surface Site Type	Crystal Face N_s (sites/nm^2)			
	(101)	(001)	(210)	(010)
≡FeO	3.03	3.34	7.5	9.1
$\equiv Fe_2O$	0	0	7.5	9.1
$\equiv Fe_3O$	3.03	3.34	0	0

Using the titration congruency method proposed by Salazar-Camacho and Villalobos [60], the potentiometric titration data of the 63 m^2/g goethite used in this research, GOE63, was compared with a second goethite sample, previously produced by Weng et al. [90], labeled HVR94 and possessing a specific surface area (SSA) of 94 m^2/g. Based on Gaboriaud's and Ehrhardt's [116] work using atomic force microscopy (AFM) imaging to characterize goethite surfaces with varying SSAs, the HVR94 goethite sample was determined to have a CFC consisting of 70% (101) crystal face and 30% (001) crystal face (using the Pnma space group) [60], [116]. Alignment of GOE63's potentiometric titration data with that of HVR94 (Figure 7) revealed a proton reactive site density value of 6.6 sites/nm^2 for GOE63. Using the N_H value of 6.6 sites/nm^2 for GOE63, and the fact that only singly and triply coordinated surface sites are considered to be proton reactive on goethite, allows for calculation of N_H.

$$N_H = \sum_k (\%\ Crystal\ Face_i)\left(N_{S,\equiv FeOH,i} + N_{s,\equiv Fe_3O,i}\right) \tag{7}$$

where N_H is in units of sites·nm^{-2}, % Crystal Face$_i$ is the percent of the mineral surface comprised from the ith crystal face, Ns,≡FeOH,$_i$ and Ns,≡Fe$_3$O,$_i$ are the site densities of singly and triply coordinated sites, respectively, present on the ith crystal face, in units of sites·nm^{-2}, and the summation is over all crystal faces k considered. The surface of the goethite sample GOE63 was considered to be comprised of some combination of the (101), (001), and (210) crystal faces:

$$1 = \sum_k (\%\ Crystal\ Face)_i \tag{8}$$

where (% Crystal Face)i is the percent of the mineral surface comprised from the ith crystal face and the summation is over all crystal faces k considered. Using Equation 8 along with GOE63's selenite surface saturation data and its proton reactive site density (N_H), the CFC of the goethite sample was estimated.

Utilizing the selenite surface saturation value observed for GOE63, along with the N_H value determined for the goethite sample, and recalling that the (101), (001), and (210) crystal faces are considered to be present on the mineral surface, the CFC of GOE63 can be estimated to be 31% (101), 55% (001), and 14% (210). This CFC is in good agreement with the findings of Gaboriaud and Ehrhardt [116] who, using AFM images, found a CFC of 30% (101) and 70% (001) for a goethite sample possessing a SSA of 49 m^2/g. Furthermore, using the CFC presented here, GOE63's predicted tritium exchange site density (N_{TRIT}) was found to be 17.0 surface protons/nm^2 which is in good agreement with the experimental and

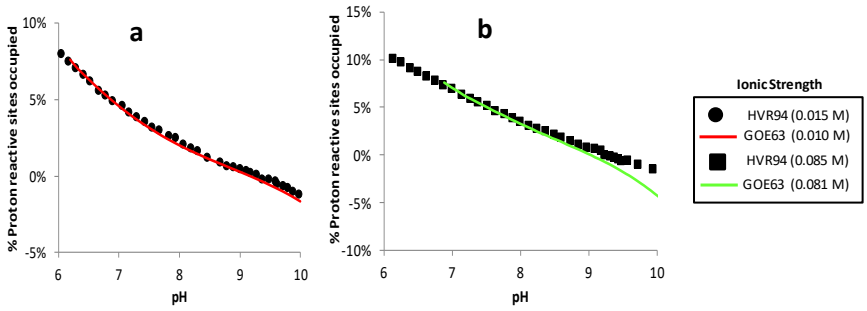

Figure 7. Fits from titration congruency method for GOE63 and HVR94 potentiometric titration data. NH for GOE63 was adjusted until the HVR94 and GOE63 data sets aligned for a given ionic strength (a) ≈ 0.01 M and (b) ≈ 0.08 M. The background electrolyte used in each case was $NaNO_3$.

theoretical values obtained by Yates et al. [142] of 16.4 ± 0.7 and 16.8 surface protons/nm^2, respectively, for goethite samples with SSAs ranging from 39 to 54 m^2/g. Hence, the resulting CFC for GOE63 provides conformity among the different site density values predicted using crystallography, microscopic image analysis, surface saturation data, surface charging data, and tritium exchange. With the CFC for GOE63 determined, the NS value for each different site type considered in the CD-MUSIC model can be calculated (Table 3).

Table 3. Site Types and N_S used in the CD-MUSIC model for GOE63.

Site Type	Crystal Face	CFC (%)	N_S (sites/nm^2)	
			Individual [a]	Model [b]
≡FeOH	(101)	31	0.94	2.79
	(010)	55	1.85	
	(210)	14	1.03	1.03
≡Fe_2OH	(101)	31	-	-
	(010)	55	-	
	(210)	14	1.03	1.03
≡Fe_3O	(101)	31	0.94	2.79
	(010)	55	1.85	
	(210)	14	-	-

[a] "Individual" Ns values were calculated for each site type by multiplying the CFC percentage by the respective crystal face's reactive site density (cf. Table 2)

[b] Values under the column labeled "model" represent the site densities used in CD-MUSIC for GOE63. For the (101) and (001) crystal faces, the Ns value for a given site type is calculated by summing the Ns values presented in the "Individual" column for the (101) and (001) faces. For the (210) crystal face, the site densities in the "model" column are equivalent to those presented in the "individual" column.

3. Estimation of capacitance

Several precedent setting studies have documented the role that the capacitance values play in predicting potentiometric titration data; there is an inverse semi-linear relationship between the SSA and capacitance

value of goethites [23], [39], [42], [45], [52], [60], [116], [140]. The current study hypothesizes that establishing a predictive method to determine capacitance values based on SSA of goethite can extend the capability of SCMs to predict proton adsorption behavior and metal ion adsorption to various preparation of goethites.

In this study, the relationship between capacitance and SSA was created by fitting multiple proton adsorption data on goethites of various SSA with the CD-MUSIC model. Titration data was collected from other studies [41], [42], [45], [109], and the capacitance value were adjusted to fit the data using FITEQL 4.0.

Titration data for four different goethite preparations was collected from literature. The specific surface area (SSA) of the goethites used in the collected data ranged from 37 m^2/g to 98.6 m^2/g. All titrations were reported to be performed in CO_2-free environments, with $NaNO_3$ as electrolytes, and with the pH_{pzc} of goethite ranging within 9.1±0.3. The data were used to establish a linear relationship between specific surface area and capacitance that was able to describe all four data sets.

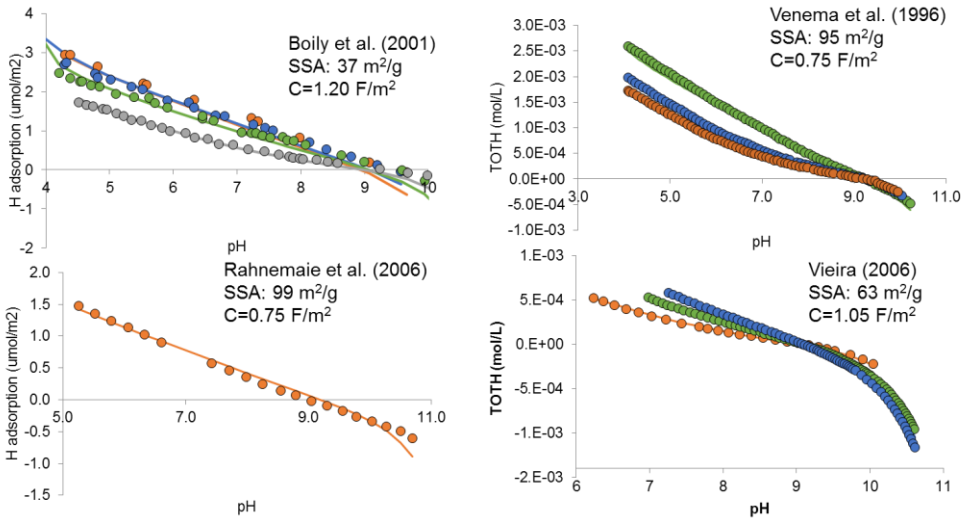

Figure 8. CD-Music modeling of titration data collected for four different specific surface area goethites.

4. Surface Complexation Modeling of Transition Metal Ions

Potentiometric titration data and pH adsorption edge data for Cd(II) from our research were used to calibrate the CD-MUSIC model while the Cd(II) isotherm adsorption data and experimental data from Venema et al. [41]were used to test the model's predictive capability. Cd(II) adsorption was modeled on goethite utilizing a tridentate edge sharing complex forming on the (210) crystal face, and a bidentate corner sharing complex and monodentate surface complex, both forming on the (101) and (001) crystal faces of goethite based on spectroscopic and DFT calculations [67], [132], [133], [143]. The resulting model fits for the pH adsorption edge experiments were satisfactory and the model proved capable of accurately predicting GOE63's Cd(II) isotherm adsorption data.

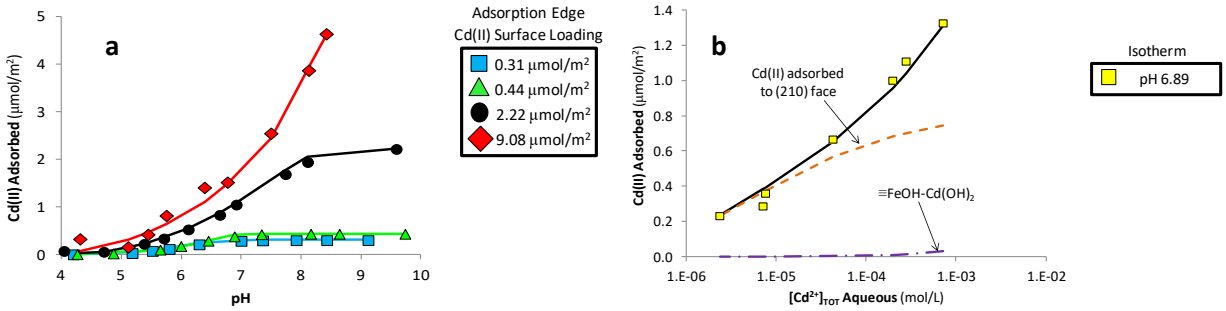

Figure 9. (a) Cd(II) pH adsorption edge data for GOE63 at four different Cd(II) surface loadings. (b) Cd(II) isotherm adsorption data for GOE63 at pH 6.89. Symbols denote experimental data points while solid lines represent model simulations of total Cd(II) adsorbed. The dashed orange line in plots (b) represents the amount of Cd(II) adsorbed to the (210) crystal face while the dotted and dashed purple line denotes the amount of Cd(II) adsorbed as the monodentate surface complex that binds via a vertex linkage to the (101) and (001) crystal faces.

Utilizing a newly proposed Pb(II) tridentate surface complex, CD-MUSIC's simulated surface speciation of Pb(II) on GOE63 is in agreement with spectroscopic findings [139], [144] over the entire pH range studied. To our knowledge, this is the first model that is capable of describing Pb(II) ion adsorption to goethite over the pH range from 3 to 11.

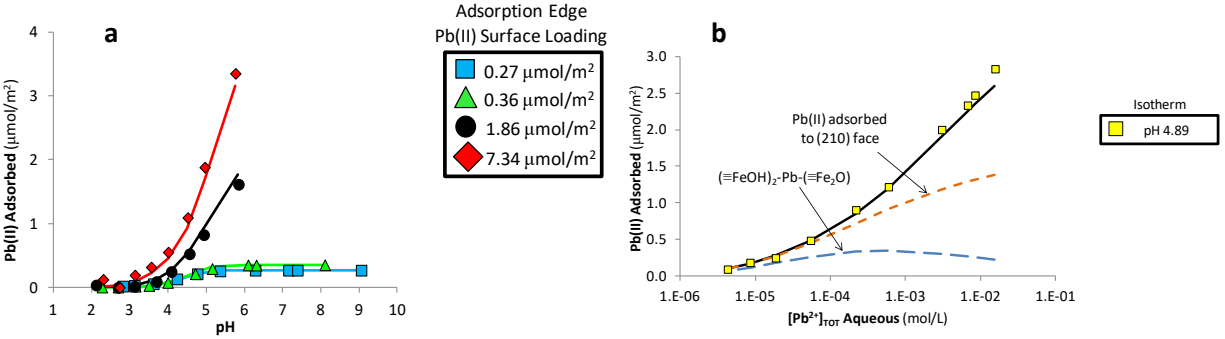

Figure 10. (a) Pb(II) pH adsorption edge data for GOE63 at four different Pb(II) surface loadings. (b) Pb(II) isotherm adsorption data for GOE63 at pH 4.89. Symbols denote experimental data points while solid lines represent model simulations of total Pb(II) adsorbed. The dashed orange line in plot (b) represents the amount of Pb(II) adsorbed to the (210) crystal face while the long dash blue line denotes the amount of Pb(II) adsorbed as the $(\equiv FeOH)_2$-Pb-$(\equiv Fe_2O)$ surface complex that binds via a corner and edge linkage to the (210) crystal face.

In Cd(II)/Pb(II) bi-solute systems, competition between the adsorbates for surface sites affects the adsorption behavior of Cd(II) relative to what is observed in single solute systems. The CD-MUSIC model developed in this study is able to predict the effects of this site competition and correctly describe the adsorption behavior of both cations in the Cd(II)/Pb(II) bi-solute system. Similar attempts to model cation/cation competition with simpler models has often lead to over prediction of the extent of competition [18].

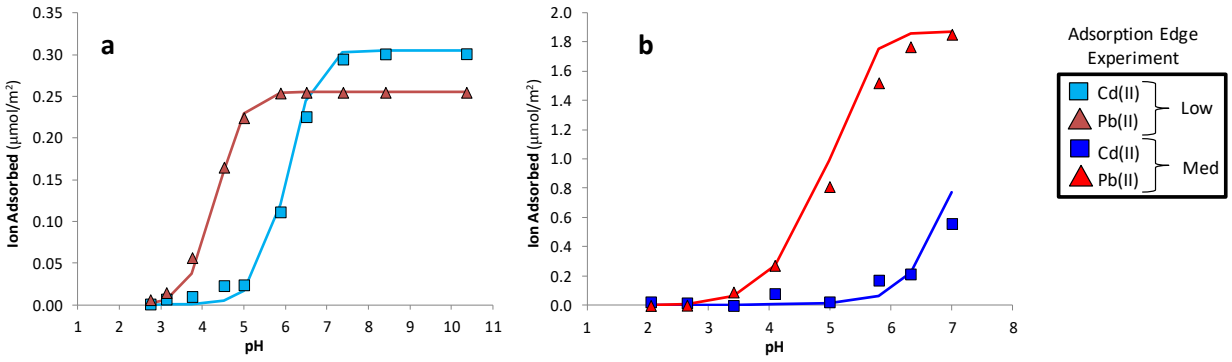

Figure 11. (a) and (b) Cd(II) and Pb(II) bi-solute pH adsorption edge data for the GOE63 goethite sample with surface loadings of (a) 0.31 and 0.26 µmol/m^2, respectively ("Low" surface loading); and (b) 2.15 and 1.87 µmol/m^2, respectively ("Medium" surface loading. In all plots, symbols denote experimental data and solid lines denote CD-MUSIC model predictions.

In both the Cd(II)/Se(IV) and Pb(II)/Se(IV) bi-solute adsorption experiments, total ion adsorption exceeded the site capacity of the goethite. In contrast to the Cd(II)/Pb(II) bi-solute system where evidence for competition was observed in Cd(II)'s adsorption edge shift (Figure 4d), comparison of single and bi-solute experimental adsorption data for the cation/oxyanion systems revealed that no reduction in sorption occurred for any of the adsorbates (i.e., Cd(II), Pb(II), and Se(IV)) considered. These differences between the cation-cation and cation-oxyanion bi-solute systems can be attributed to the reduction in charge associated with adsorption of counter-ion solutes and/or the formation of ternary complexes. Based on comparison with similar bi-solute systems (i.e., Cd(II)/S(IV) and Pb(II)/S(IV)), the formation of ternary complexes is expected. Incorporation of ternary surface complexes did lead to excellent simulations of the bi-solute data for both systems. Further confirmation of these species through molecular modeling and/or spectroscopy should be conducted to confirm the presence of these complexes within the range of conditions implicated by the modeling results.

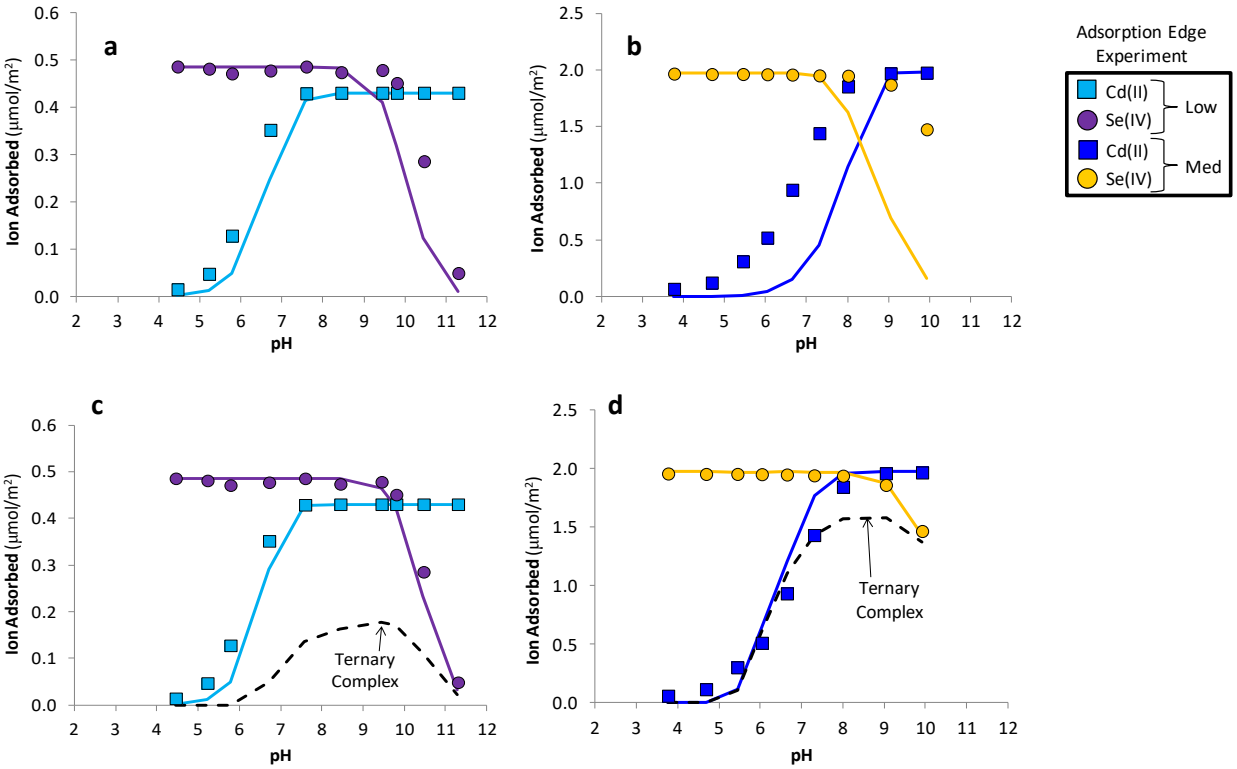

Figure 12. Cd(II) and Se(IV) bi-solute pH adsorption edge data for the GOE63 goethite sample with surface loadings of (a) and (c) 0.43 and 0.49 µmol/m^2, respectively ("Low" surface loading); and (b) and (d) 1.98 and 1.97 µmol/m^2, respectively ("Medium" surface loading). CD-MUSIC model simulations were conducted assuming ternary surface complexes were (a) and (b) absent; and (c) and (d) present. Symbols denote experimental data and solid lines denote CD-MUSIC model predictions. The black dashed line in plots (c) and (d) represents the amount of Cd(II) and Se(IV) adsorbed to the (101) and (001) crystal faces via the proposed (≡FeOH)$_2$-CdOSeO$_2$ ternary surface complex.

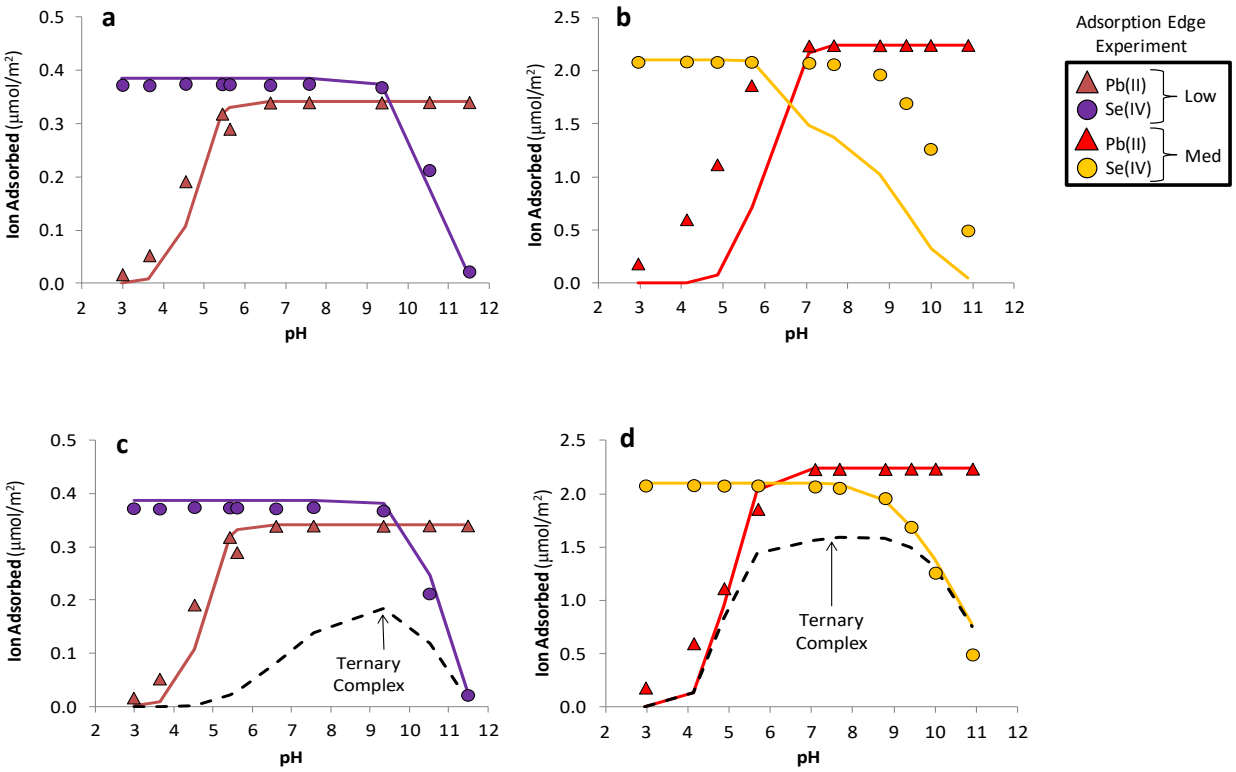

Figure 13. Pb(II) and Se(IV) bi-solute pH adsorption edge data for the GOE63 goethite sample with surface loadings of (a) and (c) 0.34 and 0.39 µmol/m^2, respectively ("Low" surface loading); and (b) and (d) 2.24 and 2.10 µmol/m^2, respectively ("Medium" surface loading). CD-MUSIC model simulations were conducted assuming ternary surface complexes were (a) and (b) absent; and (c) and (d) present. Symbols denote experimental data and solid lines denote CD-MUSIC model predictions. The black dashed line in plots (c) and (d) represents the amount of Pb(II) and Se(IV) adsorbed to the (210) crystal face via the proposed (≡FeOH)-PbOSeO$_2$-(≡Fe$_2$OH) ternary surface complex.

A summary of the surface complexation model parameters for this system is presented in Table 4.

Table 4. CD-MUSIC surface complexation model parameters for goethite

Adsorbate	Crystal Face	Surface Complex	Linkage Type	Δz_0	Δz_1	Log K_{in}
H^+	(101), (001) & (210)	$\equiv FeOH^{-0.5} + H^+ \rightarrow \equiv FeOH_2^{+0.5}$	-	1	0	8.5
		$\equiv FeOH^{-0.5} + H^+ + NO_3^- \rightarrow \equiv FeOH_2^{+0.5}\_NO_3^-$	-	1	-1	8.0
		$\equiv FeOH^{-0.5} + H^+ + Cl^- \rightarrow \equiv FeOH_2^{+0.5}\_Cl^-$	-	1	-1	8.1
		$\equiv FeOH^{-0.5} + Na^+ \rightarrow \equiv FeOH^{-0.5}\_Na^+$	-	0	1	0.1
	(101) & (001)	$\equiv Fe_3O^{-0.5} + H^+ \rightarrow \equiv Fe_3OH^{+0.5}$	-	1	0	11.7
		$\equiv Fe_3O^{-0.5} + H^+ + NO_3^- \rightarrow \equiv Fe_3OH^{+0.5}\_NO_3^-$	-	1	-1	11.2
		$\equiv Fe_3O^{-0.5} + H^+ + Cl^- \rightarrow \equiv Fe_3OH^{+0.5}\_Cl^-$	-	1	-1	11.3
		$\equiv Fe_3O^{-0.5} + Na^+ \rightarrow \equiv Fe_3O^{-0.5}\_Na^+$	-	0	1	0.1
Cd^{+2}	(101) & (001)	$2(\equiv FeOH^{-1/2}) + Cd^{+2} \rightarrow (\equiv FeOH)_2\text{-}Cd$	Corner	0.82	1.18	5.88
		$\equiv FeOH^{-1/2} + Cd^{+2} + 2H_2O \rightarrow (\equiv FeOH)\text{-}Cd(OH)_2 + 2H^+$	Vertex	0.41	-0.41	-11.96
	(210)	$2(\equiv Fe'OH^{-1/2}) + \equiv Fe_2'OH^0 + Cd^{+2} \rightarrow (\equiv Fe'OH)_2\text{-}Cd\text{-}(\equiv Fe_2'OH)$	Edge	1.15	0.85	7.31
		$2(\equiv Fe'OH^{-1/2}) + \equiv Fe_2'OH^0 + Cd^{+2} \rightarrow (\equiv Fe'OH)_2\text{-}Cd\text{-}(\equiv Fe_2'O) + H^+$	Edge	0.32	0.68	-0.90
Pb^{+2}	(101) & (001)	$\equiv FeOH^{-1/2} + Fe_3O^{-1/2} + Pb^{+2} + H_2O \rightarrow (\equiv FeO)\text{-}PbOH\text{-}(\equiv Fe_3O) + 2H^+$	Edge	0.16	-0.16	-4.13
		$2(\equiv FeOH^{-1/2}) + Fe_3O^{-1/2} + Pb^{+2} \rightarrow (\equiv FeOH)_2\text{-}Pb\text{-}(\equiv Fe_3O)$	Edge	1.49	0.51	11.83
	(210)	$\equiv Fe'OH^{-1/2} + \equiv Fe_2'OH^0 + Pb^{+2} + H_2O \rightarrow (\equiv Fe'OH)\text{-}PbOH\text{-}(\equiv Fe_2'O) + 2H^+$	Edge	0.08	-0.08	-5.60
		$2\ (\equiv Fe'OH^{-1/2}) + \equiv Fe_2'OH^0 + Pb^{+2} \rightarrow (\equiv Fe'OH)_2\text{-}Pb\text{-}(\equiv Fe_2'OH)$	Edge & Corner	1.4	0.6	10.70
SeO_3^{-2}	(101) & (001)	$2(\equiv FeOH^{-1/2}) + SeO_3^{-2} + 2H^+ \rightarrow (\equiv FeO)_2\text{-}SeO + 2H_2O$	Corner	0.75	-0.75	22.85
	(210)	$2(\equiv Fe'OH^{-1/2}) + SeO_3^{-2} + 2H^+ \rightarrow (\equiv Fe'O)_2\text{-}SeO + 2H_2O$	Corner	0.67	-0.67	23.93
		$2(\equiv Fe'OH^{-1/2}) + SeO_3^{-2} + 3H^+ \rightarrow (\equiv Fe'O)_2\text{-}SeOH + 2H_2O$	Corner	0.67	0.33	29.83
Cd^{+2} and SeO_3^{-2}	(101) & (001)	$2(\equiv FeOH^{-1/2}) + SeO_3^{-2} + Cd^{+2} \rightarrow (\equiv FeOH)_2\text{-}Cd\text{-}OSeO_2$	Corner	0.82	-0.82	13.07
Pb^{+2} and SeO_3^{-2}	(210)	$\equiv Fe'OH^{-1/2} + \equiv Fe_2'OH^0 + Pb^{+2} + SeO_3^{-2} \rightarrow (\equiv Fe'OH)\text{-}PbOSeO_2\text{-}(\equiv Fe_2'OH)$	Edge	0.92	-0.92	19.09

5. Surface Complexation Modeling of Alkaline Earth Metal Ions

The same CD-MUSIC parameters developed for the transitions metal ions was applied to model alkaline earth metal ion adsorption. The resulting surface complex species for each alkaline earth metal ion determined from the data fitting process are listed in Table 5. For Ba^{2+} and Sr^{2+}, only outer-sphere species were required to fit experimental data, whereas for Ca^{2+} and Mg^{2+}, inner-sphere species were also required. This is consistent with the observed trend from our adsorption batch experiments where Mg^{2+} and Ca^{2+} show stronger binding with the goethite surface compared to Sr^{2+} and Ba^{2+}. MeOH = species were required to fit the adsorption at high pH ranges for all alkaline earth metals except Ba. Also, as suggested by spectroscopic and molecular dynamic data, outer-sphere tetradentate species were the dominant species for Sr^{2+} and Ba^{2+}.

Table 5. CD-Music surface complex species of alkaline earth metal ions on goethite

Surface Complex Species		Charge Distribution			log K			
Formula	Description	Δz_0	Δz_1	Δz_2	Mg	Ca	Sr	Ba
≡FeOHMeOH	Inner-, Mono-	0.33	0.67	0	-3.90	-7.35		
(≡FeOH)_ Me_(≡Fe_3O)	Outer, Bi-	0	2	0				4.39
2(≡FeOH)_ Me_2(≡Fe_3O)	Outer, Tetra-	0	2	0			7.66	
4(≡Fe_3O)_Me								13.21
≡FeOH_MeOH	Outer, Mono-	0	1	0			-7.12	
4(≡FeOH)_MeOH	Outer-, Tetra-	0	1	0	-3.60	-5.29		

Based on the surface complex species described above, predictions were made for alkaline earth metal ion adsorption on goethite under various solution conditions. Figure 14 compares the model prediction with experimental data for Ca^{2+} adsorption at different surface-to-metal loading ratios for two extreme cases of 0.01M and 0.7M ionic strength. As the surface/metal ratio is reduced, it is expected that the fraction of the alkaline earth metal ion removed from solution will decrease. Also, due to the limited availability of surface sites, the proportion of tetradentate surface species will also decrease as surface/metal ratio decreases. The predictions in Figure 14 show good agreement with experimental data where the surface/metal ratio is reduced by 1/6 and 1/20 from the original value used for the data fitting. (i.e. 1.2 g/L goethite with 1E x10M Ca^{2+}, and 1.2 g/L goethite with $3.33x10^{-4}$M Ca^{2+}, respectively)

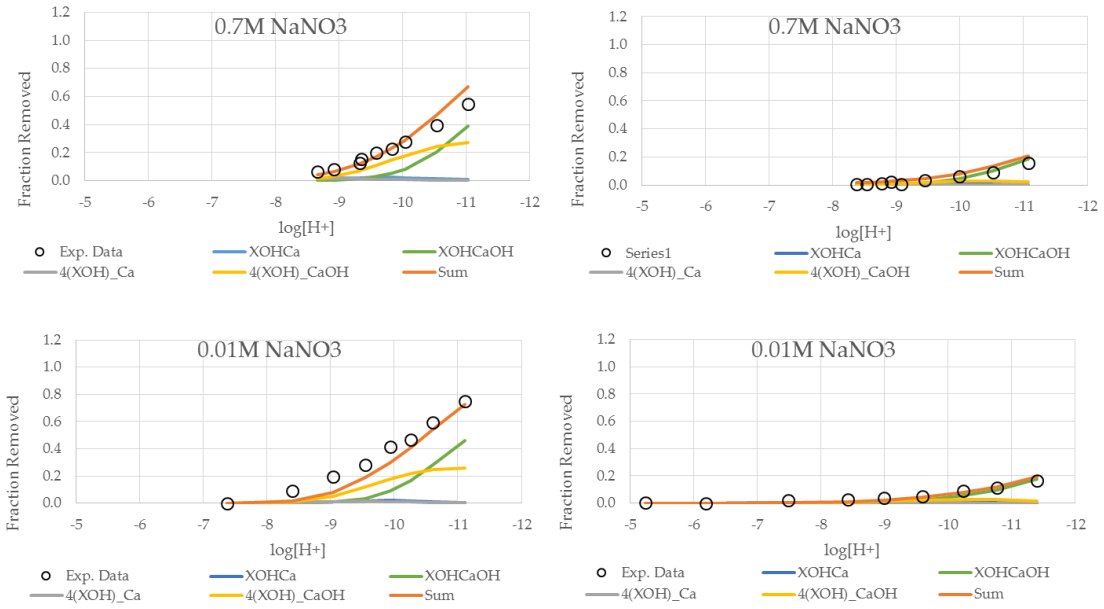

Figure 14. Experimental data and model prediction of Ca^{2+} adsorption on goethite for different surface-to-metal loadings in 0.01M and 0.7M $NaNO_3$ solutions. (a) surface/metal ratio changed to 1.2g/L goethite / $1x10^{-4}$M Ca^{2+}; (b) ratio changed to 1.2 g/L goethite / $3.33x10^{-4}$M Ca^{2+}.

Predictions were also made for electrolyte concentrations between the two extremes (0.01M and 0.7M) that were used for data fitting. Figure 15 shows four examples of modeling results: Mg^{2+} and Sr^{2+} adsorption in 0.1M and 0.3M $NaNO_3$ solutions. The agreement between the model with the experimental data demonstrates that the model is capable of predicting alkaline earth metal ion adsorption over a wide range of $NaNO_3$ concentrations which spans at least from 0.01M to 0.7M.

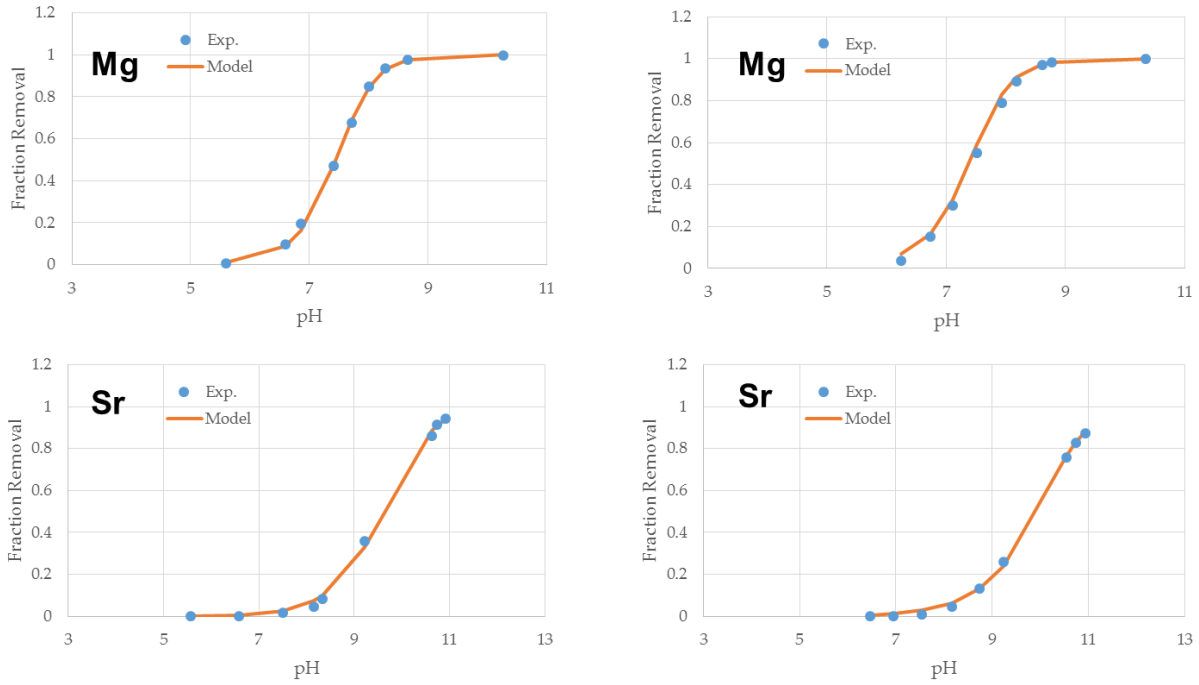

Figure 15. Predictions of Mg^{2+} and Sr^{2+} adsorption on goethite in 0.1M and 0.3M $NaNO_3$ solutions. (a) Mg^{2+} in 0.1M $NaNO_3$; (b) Mg^{2+} in 0.3M NaNO3; (c) Sr^{2+} in 0.1M $NaNO_3$; (d) Sr in 0.3M $NaNO_3$

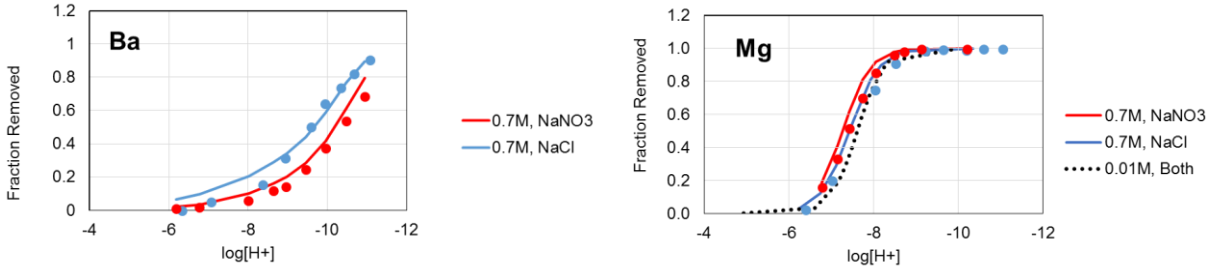

Figure 16. Predictions of Ba^{2+} and Mg^{2+} adsorption on goethite in 0.7M $NaNO_3$ and NaCl solutions

Figure 16 illustrates the modeling results of Ba and Mg adsorption on goethite in 0.7M $NaNO_3$ and NaCl solutions. As described in previous chapters, the aqueous complexation of alkaline earth metal ions with NO_3^- ligands reduces the concentration of free metal ions which consequently affects the adsorption on goethite. In comparison with $NaNO_3$ solutions, the free concentration of Ba^{2+} is higher, whereas for Mg^{2+} the uncomplexed concentration is lower in NaCl solutions. The model accurately predicted these differences in adsorption associated with different solution chemistry. The relatively small difference in Mg^{2+} adsorption between $NaNO_3$ and NaCl solution is assumed to be due to the higher surface affinity of Mg^{2+} compared to Ba^{2+}.

Model predictions of Ba^{2+} adsorption in a more complex solution system (i.e. mixture of 0.35M $NaNO_3$ and 0.35M NaCl) were also conducted. Ba^{2+} was specifically selected as the adsorbate due to its

relatively low affinity to goethite which results in greater impact on adsorption by background electrolytes. Figure 17 illustrates the agreement with the experimental data.

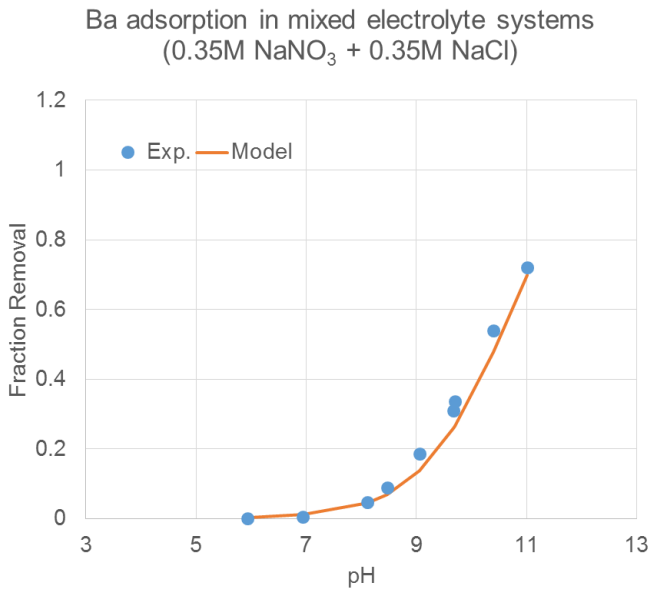

Figure 17. Experimental data and model prediction of Ba^{2+} adsorption in complex electrolyte system (mixture of 0.35M $NaNO_3$ and 0.35M NaCl).

The predictions for Ba adsorption in two different preparations of goethite (i.e. 50 m^2/g and 64.5 m^2/g) are shown in Figure 18. When the electrolyte concentration and total surface area of goethite in batch reactors are identical, Ba adsorption is observed to be greater on the 50 m^2/g goethite compared to the 64.5 m^2/g goethite. Our predictions show trends consistent with the experimental results. This provide evidence that the model developed can be extended to different preparation of goethites with different CFCs.

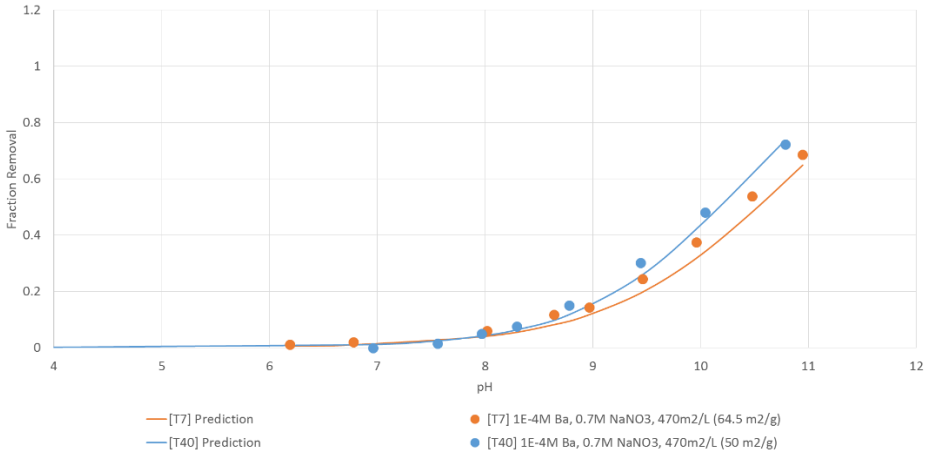

Figure 18. Experimental data and model prediction of Ba adsorption in complex electrolyte system (mixture of 0.35M $NaNO_3$ and 0.35M NaCl).

3. Products

A. Journal Articles

Choi, J. Y., Kinney, K. A., & Katz, L. E. (2016). "Effect of $CaCO_{3(S)}$ Nucleation Modes on Algae Removal from Alkaline Water." *Environmental Science & Technology,* DOI: 10.1021/acs.est.5b05255.

Mangold, J. et al., (2014) Surface Complexation Modeling of Hg(II) Adsorption at the Goethite/Water Interface using the CD-MUSIC Model, *Journal of Colloid and Interface Science,* 418(15) 147–161.

Ernst, C., Katz, L., and Barrett, M. (2015) Removal of Dissolved Copper and Zinc from Highway Runoff via Adsorption. *J. Sustainable Water Built Environ*., 10.1061/JSWBAY.0000803, 04015007.

Park, C. M., Katz, L. E., & Liljestrand, H. M. (2015). Mercury speciation during in situ thermal desorption in soil. *Journal of Hazardous Materials*, 300, 624-632.

Jubb, A., et al. (2013) Sulfate adsorption at the buried hematite/solution interface investigated using total internal reflection (TIR)-Raman spectroscopy, *Journal of Colloid and Interface Science*, 400. 140-146.

Katz, L.E. et al., (2013) Temperature effects on alkaline earth metal ions adsorption on gibbsite: Approaches from macroscopic sorption experiments and molecular dynamics simulations, *Journal of Colloid and Interface Science*, 399. 68-76

Wiesner, A.D., Katz, L.E and Chen, C.C., "The impact of ionic strength and background electrolyte on pH measurements in metal ion adsorption experiments," *Journal of Colloid and Interface Science*, Vol. 301, pp. 329-332, 2006.

Chen, C.C., Coleman, M.L. and Katz, L.E., (2006) "Bridging the Gap between Macroscopic and Spectroscopic Studies of Metal Ion Sorption at the Oxide/Water Interface: Sr(II), Co(II), and Pb(II) Sorption to Quartz," *Environmental Science & Technology,* Vol. 40, No. 1, pp. 142-148.

B. Presentations

Coleman, M.C., Chen, C.C. and Katz, L.E., "Effect of Background Electrolyte Anions on Divalent Metal Ion Sorption at the Mineral/Water Interface," presented at the American Chemical Society 227th National Meeting, Anaheim, CA, March 2004.

Vieira, A, Stokes, S.N., Chen, C.C. and Katz, L.E., "Estimation of Surface Site Density for Surface Complexation Modeling of Metal Ion Sorption onto Iron Oxides," presented at American Chemical Society 229th National Meeting, San Diego, CA, March 13-17, 2005.

Katz, L.E., Chen, C.C., Coleman, M. L. and Wiesner, A.D., "Bridging the Gap between Macroscopic and Spectroscopic Studies of Metal Ion Sorption at the Oxide/Water Interface," presented at the 79th American Chemical Society Colloid and Surface Science Symposium, Clarkson University, Potsdam, NY, June 12-15, 2005.

Vieira, A.R., Stokes, S.N., Chen, C.C. and Katz, L.E., "Comparison of Surface Complexation Models for Predicting Bi-Solute Metal Ion Sorption onto Iron Oxides," presented at 79th American Chemical Society Colloid and Surface Science Symposium, Clarkson University, Potsdam, NY, June 12-15, 2005.

Katz, L.E., "Surface Complexation Chemistry," Invited, presented at the American Water Works Association Inorganics Contaminants Workshop, Austin, TX, January 2006.

Stokes, S.N., Chen, C.C., Speitel, G.E. Jr. and Katz, L.E., "Diffuse Layer Modeling (DLM) of Arsenic Adsorption to Three Commercially Available Granular Media," presented at the American Chemical Society National Meeting in Atlanta, GA, March 26-30, 2006.

Wiesner, A.D., Chen, C.C. and Katz, L.E., "The impact of background electrolytes on metal ion adsorption: A study of Co(II) and Pb(II) partitioning at the gibbsite/water interface by microscopic and macroscopic approaches," presented at the American Chemical Society National Meeting in Atlanta, GA, March 26-30, 2006.

Katz, L. E., Chen, C.C., Stokes, S.N. and Vieira, A., "Multi-solute Removal of Metal Ions and Oxyanions on Natural and Engineered Oxide Minerals," presented at the Gordon Research Conference on Water, Holden, NH, June 2006.

Katz, Lynn E., Chen, Chia-chen, Vieira, Adriano R., Wiesner, and Andrew D. "Experimental and Modeling Approaches for Investigation of Systems Involving Metal-Anion Pairing at Solid/Water Interfaces," presented at the 232nd ACS National Meeting, San Francisco, CA, September 10-14, 2006.

Katz, Lynn E., Stokes, Shannon N., and Chen, Chia-chen. "Surface Complexation Modeling of Metal Ion Adsorption to Iron Oxides," presented at the 235th ACS National Meeting, New Orleans, LA, April 6-10, 2008.

Katz, Lynn E., Criscenti, Louise J., Chen, Chia-chen, and Larentzos, James P. "Temperature Effects on Adsorbed Alkaline-Earth-Metal Coordination Structure on Gibbsite," presented at the 235th ACS National Meeting, New Orleans, LA, April 6-10, 2008.

Lai,C.K., Katz,L. E., Liljestrand,H.M. and London, M.R. "Reactivity of Newly Synthesized Nanoscale ZVI for Perchlorate Degradation, " presented at the Remediation of Chlorinated and Recalcitrant Compounds, Monterey, CA, May 19-22, 2008.

Katz, Lynn E., Chen, Chia-chen, Speitel, Gerald E. Jr., and Stokes, Shannon N. "Modeling Metal Ion Adsorption in Packed Bed Reactor Systems," presented at the 237th ACS National Meeting, Salt Lake City, UT, March 22-26, 2009.

Criscenti, Louise J., Katz, Lynn E., and Wander, Matthew C.F. "Evaluating the Thermodynamics of Metal Ion Adsorption at the Molecular Scale," presented at the 237th ACS National Meeting, Salt Lake City, UT, March 22-26, 2009.

Mangold, Jeremiah, Chen, Chia-chen, and Katz, Lynn E. "Comparison of Surface Complexation Models for Predictions Sorption onto Goethite Surfaces," presented at the 238th ACS National Meeting, Washington, DC, August 16-20, 2009.

Criscenti, L. J., L. E. Katz, et al. (2010). Evaluating the thermodynamics of metal ion adsorption at the molecular scale, Presented at the 239th ACS National Meeting in San Francisco, CA, March 2010.

Park, Chang M.; Mangold, Jeremiah; Katz, Lynn; Liljestrand, Howard, Charge distribution multi-site complexation (CD-MUSIC) modeling of Hg(II) adsorption on goethite, 241st ACS National Meeting & Exposition, Anaheim, CA, United States, March 27-31, 2011

Choi, Jinyong; Kinney, Kerry A.; Katz, Lynn E.; Chen, Eric, pH-induced flocculation process for harvesting microalgae from water, 241st ACS National Meeting & Exposition, Anaheim, CA, United States, March 27-31, 2011

Mangold, Jeremiah E.; Katz, Lynn, Application of the CD-MUSIC model to single and multi-solute adsorption experiments using a titration congruency method for site density calculations, 241st ACS National Meeting & Exposition, Anaheim, CA, United States, March 27-31, 2011

Dozier, Celina S.; Katz, Lynn; Liljestrand, Howard, Activated alumina for the adsorption of antibiotics ciprofloxacin and oxytetracycline in the presence of natural organic matter, 241st ACS National Meeting & Exposition, Anaheim, CA, United States, March 27-31, 2011

Katz, L.E. "Geochemistry of Environmental Interfaces: Ion-pairing at Fe-oxide/water interfaces," Geochemical Probes and Processes Symposium, Gaithersburg, MD, March, 2013

Katz, L.E., Ernst, C., Han, J.K., Wessling, T. and Barrett, M., "Removal of Dissolved Heavy Metals in Highway Runoff," International Symposium on Rainwater Utilization, July 1-July 4, 2013, Beijing/Nanjing, China (Invited)

Katz, Lynn E.; Mangold, Jeremiah E.; Choi, Jin Yong; Ernst, Clayton O.; Han, Joon; Barrett, Michael E. Application of molecular scale interpretations of sorption phenomena to the development of treatment and remediation processes 247th ACS National Meeting & Exposition, Dallas, TX, United States, March 16-20, 2014 (Invited)

F.A. Diaz, L.E. Katz, D.F. Lawler, (2015) Binding of inorganic mercury in surface water to DOM and alum flocs: How much removal can we get?, Presented at the ACS National Meeting, Denver, CO, March 22-26, 2015

C. Dozier, L.E. Katz, H. Liljestrand (2015) Application of molecular scale interpretations of sorption phenomena to the development of treatment and remediation processes.. Presented at the American Chemical Society National Meeting, Denver, CO. March 22-26

J. Han, S. Chun, L.E. Katz (2015) Characterization of Ba2+ adsorption on oxide minerals: Combined effects of solution and surface properties in complex systems. Presented at the American Chemical Society National Meeting, Denver, CO. March 22-26

L.E. Katz, J. Choi, J. Han, L.J. Criscenti (Invited) (2015) Alkaline earth metal ion sorption processes: From adsorption to precipitation. Presented at the American Chemical Society National Meeting, Denver, CO. March 22-26.

L.E. Katz, K.A. Alfredo, M. Bartolo, I. Gee, J. Herrboldt, D. Lawler (Invited) (2015) Impact of ligands on co-precipitation and adsorption with aluminum hydroxide. Presented at the American Chemical Society National Meeting, Boston, MA. August 16-20

C. Dozier, L.E. Katz, H. Liljestrand (2015) Application of molecular scale interpretations of sorption phenomena to the development of treatment and remediation processes.. Presented at the American Chemical Society National Meeting, Denver, CO. March 22-26

L.E. Katz, D.F. Lawler, K. Alfredo, M. Stehouwer, C. Ernst (2015) Mechanisms of fluoride removal: Adsorption and co-precipitation with aluminum hydroxide in the presence and absence of NOM... Presented at the American Chemical Society National Meeting, Denver, CO. March 22-26

J. Han, L.E. Katz (2015) Prediction of alkaline earth metal ion adsorption on goethite for various background electrolytes. Presented at the American Chemical Society National Meeting, San Diego, CA March 13-17.

L. Criscenti, K. Leung and L. Katz (2016) Adsorption of divalent metals and oxyanions to goethite-water interfaces. Presented at the American Chemical Society National Meeting, San Diego, CA March 13-17.

J. Han, L.E. Katz (2016) Effect of metal oxides on precipitation of struvite in synthetic livestock manure and human urine. Presented at the American Chemical Society National Meeting, San Diego, CA March 13-17.

M. Bartolo, L. Katz, S. Myneni, D. Lawler, I. Gee and J. Herboldt (2016) Aluminum hydroxide, fluoride, and NOM: Insights using infrared spectroscopy. Presented at the American Chemical Society National Meeting, San Diego, CA March 13-17.

C. Ph.D. Dissertations

Dozier, Celina, May 2016 “Alumina-Titania Particles for the Heterogeneous Photocatalytic Oxidation of Ciprofloxacin” University of Texas, Austin, TX

Choi, Jinyong, August 2014 “pH-induced flocculation/deflocculation process for harvesting microalgae from water” University of Texas, Austin, TX

Mangold, Jeremiah, Dec., 2013 – completed all requirements during grace period in Aug, 2013, “Predicting Ion Adsorption onto the Iron Hydroxide Goethite in Single and Multi-Solute Systems” University of Texas, Austin, TX

Park, Chang-Min, Dec. 2009, “Mercury Speciation During Thermal Remediation and Post-Treatment Environments” University of Texas, Austin, TX

Stokes, Shannon – December 2009, “Diffuse Layer Modeling on Iron Oxides – Single and Multi-solute Systems on Ferrihydrite and Granular Ferric Hydroxide” University of Texas, Austin, TX

Adriano Vieira, May 2006, “Surface Complexation Modeling of Ph(II), Cd(II) and Se(IV), onto Iron Hydroxides in Single and Bisolute Systems” University of Texas, Austin, TX

D. M.S. Theses/Report

Sherer, Hugh, Dec. 2014 “The Effects of Ionic Strength on the Adsorption of Alkaline Earth Metals on Goethite”

Chun, Seunghwan, May 2015 “Removal of Barium with Adsorption onto MnO2”

Lynch, Christine August, 2012, “Adsorption of Cu(II) and Zn(II) onto Iron Oxide Media in Semi-Synthetic Stormwater”

Weisner, Andrew D., August 2006, ”Effects of pH Measurement on the Prediction of Surface Complexation Reactions in High Ionic Strength Solutions”

Lin, Hsiu-Chuan., August 2007. “Effects of Temperature and Ionic Strength on the Adsorption of Strontium onto Gibbsite.”

Coleman, Michael, May 2004, “Sorption Behavior of Representative Divalent Cations onto Quarter under Varying Electrolyte Conditions”

4. References

[1] D. L. Dugger, J. H. Stanton, B. N. Irby, B. L. McConnell, W. W. Cummings, and R. W. Maatman, “The Exchange of Twenty Metal Ions with the Weakly Acidic Silanol Group of Silica Gel1, 2,” *The Journal of Physical Chemistry*, vol. 68, no. 4, pp. 757–760, 1964.

[2] P. W. Schindler, B. Fürst, R. Dick, and P. U. Wolf, “Ligand properties of surface silanol groups. I. surface complex formation with Fe3+, Cu2+, Cd2+, and Pb2+,” *Journal of Colloid and Interface Science*, vol. 55, no. 2, pp. 469–475, 1976.

[3] W. Stumm, R. Kummert, and L. Sigg, “A ligand-exchange model for the adsorption of inorganic and organic-ligands at hydrous oxide interfaces,” *Croatica chemica acta*, vol. 53, no. 2, pp. 291–312, 1980.

[4] G. Sposito, “The surface chemistry of soils,” 1984.

[5] J. A. Davis and D. B. Kent, “Waste Isolation Pilot Plant Compliance Certification Application Reference 583,” *Reviews in Mineralogy and Geochemistry*, vol. 23, pp. 177–260, 1990.

[6] G. Sposito, *The chemistry of soils*, 2nd ed. Oxford university press, 2008.

[7] N. J. Barrow and V. C. Cox, “The effects of pH and chloride concentration on mercury sorption. I. By goethite,” *European Journal of Soil Science*, vol. 43, no. 2, pp. 295–304, 1992.

[8] D. A. Dzombak and F. M. M. Morel, *Surface complexation modeling: hydrous ferric oxide*. John Wiley & Sons, 1990.

[9] C.-P. Huang and W. Stumm, “Specific adsorption of cations on hydrous γ-Al< sub> 2</sub> O< sub> 3</sub>,” *Journal of Colloid and Interface Science*, vol. 43, no. 2, pp. 409–420, 1973.

[10] W. Stumm, C.-P. Huang, and S. R. Jenkins, “Specific chemical interaction affecting stability of dispersed systems,” *Croatica Chemica Acta*, vol. 42, no. 2, p. 223, 1970.

[11] H. Hohl and W. Stumm, “Interaction of Pb2+ with hydrous γ-Al2O3,” *Journal of Colloid and Interface Science*, vol. 55, no. 2, pp. 281–288, 1976.

[12] P. von Schindler and H. R. Kamber, “Die acidität von silanolgruppen. Vorläufige mitteillung,” *Helvetica Chimica Acta*, vol. 51, no. 7, pp. 1781–1786, 1968.

[13] P. W. Schindler and H. Gamsjäger, “Acid—base reactions of the TiO 2 (Anatase)—water interface and the point of zero charge of TiO 2 suspensions,” *Colloid & Polymer Science*, vol. 250, no. 7, pp. 759–763, 1972.

[14] W. Stumm, H. Hohl, and F. Dalang, “Interaction of metal-ions with hydrous oxide surfaces,”

Croatica Chemica Acta, vol. 48, no. 4, pp. 491–504, 1976.
[15] J. A. Davis, R. O. James, and J. O. Leckie, "Surface ionization and complexation at the oxide/water interface: I. Computation of electrical double layer properties in simple electrolytes," *Journal of colloid and interface science*, vol. 63, no. 3, pp. 480–499, 1978.
[16] J. A. Davis and J. O. Leckie, "Surface ionization and complexation at the oxide/water interface II. Surface properties of amorphous iron oxyhydroxide and adsorption of metal ions," *Journal of Colloid and Interface Science*, vol. 67, no. 1, pp. 90–107, 1978.
[17] J. A. Davis and J. O. Leckie, "Surface ionization and complexation at the oxide/water interface. 3. Adsorption of anions," *Journal of Colloid and Interface Science*, vol. 74, no. 1, pp. 32–43, 1980.
[18] K. F. Hayes and J. O. Leckie, "Modeling ionic strength effects on cation adsorption at hydrous oxide/solution interfaces," *Journal of Colloid and Interface Science*, vol. 115, no. 2, pp. 564–572, 1987.
[19] M. A. Blesa, A. J. G. Maroto, and A. E. Regazzoni, "Boric acid adsorption on magnetite and zirconium dioxide," *Journal of colloid and interface science*, vol. 99, no. 1, pp. 32–40, 1984.
[20] K. F. Hayes and J. O. Leckie, "Mechanism of lead ion adsorption at the goethite—water interface," ACS Publications, 1986.
[21] K. F. Hayes, C. Papelis, and J. O. Leckie, "Modeling ionic strength effects on anion adsorption at hydrous oxide/solution interfaces," *Journal of Colloid and Interface Science*, vol. 125, no. 2, pp. 717–726, 1988.
[22] D. A. Sverjensky, "Prediction of the speciation of alkaline earths adsorbed on mineral surfaces in salt solutions," *Geochimica et Cosmochimica Acta*, vol. 70, no. 10, pp. 2427–2453, May 2006.
[23] D. A. Sverjensky, "Prediction of surface charge on oxides in salt solutions: Revisions for 1:1 (M+L−) electrolytes," *Geochimica et Cosmochimica Acta*, vol. 69, no. 2, pp. 225–257, Jan. 2005.
[24] T. Hiemstra and W. H. van Riemsdijk, "A Surface Structural Approach to Ion Adsorption: The Charge Distribution (CD) Model," *Journal of Colloid and Interface Science*, vol. 179, no. 2, pp. 488–508, 1996.
[25] T. Hiemstra, J. C. M. De Wit, and W. H. van Riemsdijk, "Multisite proton adsorption at the soil/solution interface of (Hydr) oxides: a new approach. II: Application to various important (Hydr) oxides," *Journal of colloid and interface science*, vol. 133, no. 1, pp. 105–117, 1989.
[26] T. Hiemstra, W. H. van Riemsdijk, and G. H. Bolt, "Multisite proton adsorption modeling at the solid/solution interface of (hydr) oxides: A new approach: I. Model description and evaluation of intrinsic reaction constants," *Journal of colloid and interface science*, vol. 133, no. 1, pp. 91–104, 1989.
[27] G. A. Parks and P. L. DeBruyn, "The Zero Point of Charge of Oxides1," *The Journal of Physical Chemistry*, vol. 66, no. 6, pp. 967–973, 1962.
[28] J. Lützenkirchen, J. F. Boily, L. Lövgren, and S. Sjöberg, "Limitations of the potentiometric titration technique in determining the proton active site density of goethite surfaces," *Geochimica et Cosmochimica Acta*, vol. 66, no. 19, pp. 3389–3396, 2002.
[29] B. B. Johnson, "Effect of pH, temperature, and concentration on the adsorption of cadmium on goethite," *Environmental Science & Technology*, vol. 24, no. 1, pp. 112–118, 1990.
[30] C. J. Daughney and J. B. Fein, "The Effect of Ionic Strength on the Adsorption of H+, Cd2+, Pb2+, and Cu2+ byBacillus subtilisandBacillus licheniformis: A Surface Complexation Model," *Journal of Colloid and Interface Science*, vol. 198, no. 1, pp. 53–77, 1998.
[31] J.-F. Boily and J. B. Fein, "Experimental study of cadmium-citrate co-adsorption onto α-Al 2 O 3," *Geochimica et cosmochimica acta*, vol. 60, no. 16, pp. 2929–2938, 1996.
[32] U. Hoins, L. Charlet, and H. Sticher, "Ligand effect on the adsorption of heavy metals : The Sulfate - Cadmium - Goethite Case," *Water, Air, and Soil Pollution*, vol. 68, pp. 241–255, 1993.
[33] L. Lövgren, S. Sjöberg, and P. W. Schindler, "Acid/base reactions and Al (III) complexation at the surface of goethite," *Geochimica et Cosmochimica Acta*, vol. 54, no. 5, pp. 1301–1306, 1990.
[34] U. Hoins, "Zur Schwermetall-Adsorption an oxidischen Oberflächen." 1991.
[35] N. Marmier, J. Dumonceau, J. Chupeau, and F. Fromage, "Comparative-study of trivalent

lanthanide ions sorption on hematite and goethite," *COMPTES RENDUS DE L ACADEMIE DES SCIENCES SERIE II*, vol. 317, no. 12, pp. 1561–1567, 1993.
[36] S. Pivovarov, "Acid–base properties and heavy and alkaline earth metal adsorption on the oxide–solution interface: Non-electrostatic model," *Journal of colloid and interface science*, vol. 206, no. 1, pp. 122–130, 1998.
[37] K. F. Hayes, G. Redden, W. Ela, and J. O. Leckie, "Surface complexation models: An evaluation of model parameter estimation using FITEQL and oxide mineral titration data," *Journal of Colloid and Interface Science*, vol. 142, no. 2, pp. 448–469, 1991.
[38] R. O. James and G. A. Parks, "Characterization of aqueous colloids by their electrical double-layer and intrinsic surface chemical properties," in *Surface and colloid science*, Springer, 1982, pp. 119–216.
[39] M. Villalobos, M. a Trotz, and J. O. Leckie, "Variability in goethite surface site density: evidence from proton and carbonate sorption," *Journal of Colloid and Interface Science*, vol. 268, no. 2, pp. 273–287, Dec. 2003.
[40] C. Tadanier and M. Eick, "Formulating the Charge-distribution Multisite Surface Complexation Model," *Soil Science Society of America Journal*, pp. 1505–1517, 2002.
[41] P. Venema, T. Hiemstra, and W. H. van Riemsdijk, "Multisite Adsorption of Cadmium on Goethite," *Journal of colloid and interface science*, vol. 183, pp. 515–27, 1996.
[42] R. Rahnemaie, T. Hiemstra, and W. H. Van Riemsdijk, "A new surface structural approach to ion adsorption: Tracing the location of electrolyte ions," *Journal of Colloid and Interface Science*, vol. 293, pp. 312–321, 2006.
[43] T. Hiemstra and W. H. van Riemsdijk, "Physical chemical interpretation of primary charging behaviour of metal (hydr) oxides," *Colloids and surfaces*, vol. 59, pp. 7–25, 1991.
[44] T. Hiemstra and W. H. Van Riemsdijk, "On the relationship between charge distribution, surface hydration, and the structure of the interface of metal hydroxides," *Journal of Colloid and Interface Science*, vol. 301, pp. 1–18, 2006.
[45] J. F. Boily, J. Lützenkirchen, O. Balmes, J. Beattie, and S. Sjöberg, "Modeling proton binding at the goethite (a -FeOOH)– water interface," *Colloids and Surfaces A: Physicochemical and Engineering Aspects*, vol. 179, pp. 11–27, 2001.
[46] T. Hiemstra, P. Venema, and W. H. van Riemsdijk, "Intrinsic Proton Affinity of Reactive Surface Groups of Metal (Hydr)oxides: The Bond Valence Principle," *Journal of colloid and interface science*, vol. 184, pp. 680–92, 1996.
[47] J. H. A. Pieper and D. A. De Vooys, "Direct measurement of the double layer capacity at the silver iodide-aqueous electrolyte interface," *Journal of Electroanalytical Chemistry and Interfacial Electrochemistry*, vol. 53, pp. 243–252, 1974.
[48] T. Hiemstra, R. P. J. J. Rietra, and W. H. Van Riemsdijk, "Surface Complexation of Selenite on Goethite: MO/DFT Geometry and Charge Distribution," *Croatica Chemica Acta*, vol. 80, no. 2007, pp. 313–324, 2007.
[49] R. Rahnemaie, T. Hiemstra, and W. H. van Riemsdijk, "Carbonate adsorption on goethite in competition with phosphate.," *Journal of colloid and interface science*, vol. 315, no. 2, pp. 415–25, Nov. 2007.
[50] R. Rahnemaie, T. Hiemstra, and W. H. Van Riemsdijk, "Geometry, charge distribution, and surface speciation of phosphate on goethite," *Langmuir*, vol. 23, no. 7, pp. 3680–3689, 2007.
[51] T. Hiemstra, M. O. Barnett, and W. H. van Riemsdijk, "Interaction of silicic acid with goethite," *Journal of Colloid and Interface Science*, vol. 310, no. 1, pp. 8–17, 2007.
[52] J. Lützenkirchen, J. F. Boily, L. Gunneriusson, L. Lövgren, and S. Sjöberg, "Protonation of different goethite surfaces-Unified models for NaNO3 and NaCl media," *Journal of Colloid and Interface Science*, vol. 317, no. 1, pp. 155–165, 2008.
[53] M. Villalobos, M. a. Cheney, and J. Alcaraz-Cienfuegos, "Goethite surface reactivity: II. A microscopic site-density model that describes its surface area-normalized variability," *Journal of Colloid and Interface Science*, vol. 336, no. 2, pp. 412–422, 2009.

[54] P. Venema, “Charging and ion adsorption behaviour of different iron (hydr) oxides.” Landbouwuniversiteit Wageningen, 1997.
[55] K. F. Hayes, A. L. Roe, G. E. Brown, and K. O. Hodgson, “In situ X-ray absorption study of surface complexes: Selenium oxyanions on α-FeOOH,” *Science*, vol. 238, no. 4828, pp. 783–786, 1987.
[56] R. P. J. J. Rietra, T. Hiemstra, and W. H. van Riemsdijk, “Sulfate Adsorption on Goethite.,” *Journal of colloid and interface science*, vol. 218, pp. 511–521, 1999.
[57] T. Hiemstra, R. Rahnemaie, and W. H. van Riemsdijk, “Surface complexation of carbonate on goethite: IR spectroscopy, structure and charge distribution.,” *Journal of colloid and interface science*, vol. 278, no. 2, pp. 282–90, Oct. 2004.
[58] M. Ponthieu, F. Juillot, T. Hiemstra, W. H. Van Riemsdijk, and M. F. Benedetti, “Metal ion binding to iron oxides,” *Geochimica Et Cosmochimica Acta*, vol. 70, no. 11, pp. 2679–2698, 2006.
[59] M. Villalobos and J. O. Leckie, “Surface Complexation Modeling and FTIR Study of Carbonate Adsorption to Goethite.,” *Journal of colloid and interface science*, vol. 235, no. 1, pp. 15–32, Mar. 2001.
[60] C. Salazar-Camacho and M. Villalobos, “Goethite surface reactivity: III. Unifying arsenate adsorption behavior through a variable crystal face – Site density model,” *Geochimica et Cosmochimica Acta*, vol. 74, no. 8, pp. 2257–2280, 2010.
[61] T. Hiemstra and W. H. van Riemsdijk, “Fluoride Adsorption on Goethite in Relation to Different Types of Surface Sites.,” *Journal of colloid and interface science*, vol. 225, no. 1, pp. 94–104, 2000.
[62] P. Bonnissel-Gissinger, M. Alnot, J.-P. Lickes, J.-J. Ehrhardt, and P. Behra, “Modeling the adsorption of mercury (II) on (hydr) oxides II: α-FeOOH (goethite) and amorphous silica,” *Journal of colloid and interface science*, vol. 215, no. 2, pp. 313–322, 1999.
[63] T. Hiemstra and W. H. Van Riemsdijk, “Surface structural ion adsorption modeling of competitive binding of oxyanions by metal (hydr) oxides,” *Journal of Colloid and Interface Science*, vol. 210, no. 1, pp. 182–193, 1999.
[64] M. Stachowicz, T. Hiemstra, and W. H. van Riemsdijk, “Multi-competitive interaction of As(III) and As(V) oxyanions with Ca(2+), Mg(2+), PO(3-)(4), and CO(2-)(3) ions on goethite.,” *Journal of colloid and interface science*, vol. 320, no. 2, pp. 400–14, Apr. 2008.
[65] M. Kanematsu, T. M. Young, K. Fukushi, P. G. Green, and J. L. Darby, “Arsenic (III, V) adsorption on a goethite-based adsorbent in the presence of major co-existing ions: Modeling competitive adsorption consistent with spectroscopic and molecular evidence,” *Geochimica et Cosmochimica Acta*, vol. 106, pp. 404–428, 2013.
[66] T. Hiemstra, W. H. Van Riemsdijk, A. Rossberg, and K. U. Ulrich, “A surface structural model for ferrihydrite II: Adsorption of uranyl and carbonate,” *Geochimica et Cosmochimica Acta*, vol. 73, no. 15, pp. 4437–4451, 2009.
[67] P. Venema, T. Hiemstra, and W. H. van Riemsdijk, “Interaction of Cadmium with Phosphate on Goethite,” *Journal of Colloid and Interface Science*, vol. 192, no. 1, pp. 94–103, 1997.
[68] M. M. Benjamin and J. O. Leckie, “Multiple-site adsorption of Cd, Cu, Zn, and Pb on amorphous iron oxyhydroxide,” *Journal of Colloid and Interface Science*, vol. 79, no. 1, pp. 209–221, 1981.
[69] C. E. Cowan, J. M. Zachara, and C. T. Resch, “Cadmium adsorption on iron oxides in the presence of alkaline-earth elements,” *Environmental Science & Technology*, vol. 25, no. 3, pp. 437–446, 1991.
[70] S. Kuo and B. L. McNeal, “Effects of pH and phosphate on cadmium sorption by a hydrous ferric oxide,” *Soil Science Society of America Journal*, vol. 48, no. 5, pp. 1040–1044, 1984.
[71] P. J. Swedlund, J. G. Webster, and G. M. Miskelly, “Goethite adsorption of Cu (II), Pb (II), Cd (II), and Zn (II) in the presence of sulfate: properties of the ternary complex,” *Geochimica et Cosmochimica Acta*, vol. 73, no. 6, pp. 1548–1562, 2009.
[72] J. R. Bargar, G. E. Brown, and G. A. Parks, “Surface complexation of Pb (II) at oxide-water interfaces: III. XAFS determination of Pb (II) and Pb (II)-chloro adsorption complexes on goethite

and alumina," *Geochimica et Cosmochimica Acta*, vol. 62, no. 2, pp. 193–207, 1998.
[73] J. D. Ostergren, T. P. Trainor, J. R. Bargar, G. E. Brown, and G. A. Parks, "Inorganic ligand effects on Pb (II) sorption to goethite (α-FeOOH): I. Carbonate," *Journal of Colloid and Interface Science*, vol. 225, no. 2, pp. 466–482, 2000.
[74] E. J. Elzinga, D. Peak, and D. L. Sparks, "Spectroscopic studies of Pb (II)-sulfate interactions at the goethite-water interface," *Geochimica et Cosmochimica Acta*, vol. 65, no. 14, pp. 2219–2230, 2001.
[75] C. S. Kim, J. J. Rytuba, and G. E. Brown, "EXAFS study of mercury (II) sorption to Fe-and Al-(hydr) oxides: II. Effects of chloride and sulfate," *Journal of Colloid and Interface Science*, vol. 270, no. 1, pp. 9–20, 2004.
[76] E. J. Elzinga and R. Kretzschmar, "In situ ATR-FTIR spectroscopic analysis of the co-adsorption of orthophosphate and Cd (II) onto hematite," *Geochimica et Cosmochimica Acta*, vol. 117, pp. 53–64, 2013.
[77] C. N. Durfor and E. Becker, "Geological Survey Water-Supply Paper 1812," Washington D.C., 1964.
[78] D. K. Todd and L. W. Mays, "Groundwater hydrology," 1980.
[79] E. Tipping, "Modeling the competition between alkaline earth cations and trace metal species for binding by humic substances," *Environmental Science & Technology*, vol. 27, no. 3, pp. 520–529, 1993.
[80] R. Mandal, M. S. A. Salam, J. Murimboh, N. M. Hassan, C. L. Chakrabarti, M. H. Back, and D. C. Gregoire, "Competition of Ca(II) and Mg(II) with Ni(II) for binding by a well-characterized fulvic acid in model solutions," *Environmental Science & Technology*, vol. 34, no. 11, pp. 2201–2208, 2000.
[81] T. Harter, "Groundwater Quality and Groundwater Pollution," 2003.
[82] L. Candela and I. Morell, "Basic Chemical Principles of Groundwater," in *Groundwater*, vol. II, L. Silveira and E. J. Usunoff, Eds. EOLSS Publications, 2009, pp. 43–54.
[83] K. B. Gregory, R. D. Vidic, and D. a. Dzombak, "Water management challenges associated with the production of shale gas by hydraulic fracturing," *Elements*, vol. 7, pp. 181–186, 2011.
[84] J. I. Drever, "The Geochemistry of Natural Waters: Surface and Groundwater Environments, 436 pp." Prentice Hall, Upper Saddle River, NJ, 1997.
[85] M. Sajih, N. D. Bryan, F. R. Livens, D. J. Vaughan, M. Descostes, V. Phrommavanh, J. Nos, and K. Morris, "Adsorption of radium and barium on goethite and ferrihydrite: A kinetic and surface complexation modelling study," *Geochimica et Cosmochimica Acta*, vol. 146, pp. 150–163, Dec. 2014.
[86] R. Rahnemaie, T. Hiemstra, and W. H. van Riemsdijk, "Inner- and outer-sphere complexation of ions at the goethite-solution interface.," *Journal of colloid and interface science*, vol. 297, no. 2, pp. 379–388, May 2006.
[87] R. P. J. J. Rietra, T. Hiemstra, and W. H. van Riemsdijk, "Interaction between calcium and phosphate adsorption on goethite.," *Environmental science & technology*, vol. 35, no. 16, pp. 3369–74, Aug. 2001.
[88] L. P. Weng, W. H. Van Riemsdijk, and T. Hiemstra, "Cu2+ and Ca2+adsorption to goethite in the presence of fulvic acids," *Geochimica et Cosmochimica Acta*, vol. 72, no. 24, pp. 5857–5870, 2008.
[89] M. a. Ali and D. a. Dzombak, "Effects of simple organic acids on sorption of Cu2+ and Ca2+ on goethite," *Geochimica et Cosmochimica Acta*, vol. 60, no. 2, pp. 291–304, 1996.
[90] L. P. Weng, L. K. Koopal, T. Hiemstra, J. C. L. Meeussen, and W. H. Van Riemsdijk, "Interactions of calcium and fulvic acid at the goethite-water interface," *Geochimica et Cosmochimica Acta*, vol. 69, no. 2, pp. 325–339, 2005.
[91] C. R. Collins, D. M. Sherman, and K. V. Ragnarsdöttir, "The adsorption mechanism of Sr2+ on the surface of goethite," *Radiochimca Acta*, vol. 81, no. 4, pp. 201–206, 1998.
[92] N. Sahai, S. A. Carroll, S. K. Roberts, and P. A. O'Day, "X-Ray Absorption Spectroscopy of

Strontium(II) Coordination: II. Sorption and Precipitation at Kaolinite, Amorphous Silica, and Goethite Surfaces," *Journal of colloid and interface science*, vol. 222, no. 2, pp. 198–212, Feb. 2000.

[93] K. F. Hayes and L. E. Katz, "Application of X-ray absorption spectroscopy for surface complexation modeling of metal ion sorption," in *Physics and chemistry of mineral surfaces*, CRC Press: Boca Raton, FL, 1996, pp. 147–223.

[94] S. A. Carroll, S. K. Roberts, L. J. Criscenti, and P. A. O'Day, "Surface complexation model for strontium sorption to amorphous silica and goethite.," *Geochemical transactions*, vol. 9, p. 2, Jan. 2008.

[95] L. E. Katz, L. J. Criscenti, C. Chen, J. P. Larentzos, and H. M. Liljestrand, "Temperature effects on alkaline earth metal ions adsorption on gibbsite: approaches from macroscopic sorption experiments and molecular dynamics simulations.," *Journal of colloid and interface science*, vol. 399, pp. 68–76, Jun. 2013.

[96] C.-C. Chen, M. L. Coleman, and L. E. Katz, "Bridging the Gap between Macroscopic and Spectroscopic Studies of Metal Ion Sorption at the Oxide/Water Interface: Sr(II), Co(II), and Pb(II) Sorption to Quartz," *Environmental Science & Technology*, vol. 40, no. 1, pp. 142–148, Jan. 2006.

[97] P. Fenter, L. Cheng, S. Rihs, M. L. Machesky, M. J. Bedzyk, and N. C. Sturchio, "Electrical Double-Layer Structure at the Rutile-Water Interface as Observed in Situ with Small-Period X-Ray Standing Waves.," *Journal of colloid and interface science*, vol. 225, pp. 154–165, 2000.

[98] M. L. Machesky, D. J. Wesolowski, J. Rosenqvist, M. Předota, L. Vlcek, M. K. Ridley, V. Kohli, Z. Zhang, P. Fenter, P. T. Cummings, S. N. Lvov, M. Fedkin, V. Rodriguez-Santiago, J. D. Kubicki, and A. Bandura, "Comparison of cation adsorption by isostructural rutile and cassiterite.," *Langmuir : the ACS journal of surfaces and colloids*, vol. 27, no. 8, pp. 4585–93, Apr. 2011.

[99] Z. Zhang, P. Fenter, L. Cheng, N. C. Sturchio, M. J. Bedzyk, M. Předota, A. Bandura, J. D. Kubicki, S. N. Lvov, P. T. Cummings, a. a. Chialvo, M. K. Ridley, P. Bénézeth, L. Anovitz, D. A. Palmer, M. L. Machesky, and D. J. Wesolowski, "Ion adsorption at the rutile-water interface: Linking molecular and macroscopic properties," *Langmuir*, vol. 20, no. 5, pp. 4954–4969, 2004.

[100] M. Předota, Z. Zhang, P. Fenter, D. J. Esolowski, and P. T. Cummings, "Electric double layer at the rutile (110) surface. 2. Adsorption of ions from molecular dynamics and X-ray experiments," *The Journal of Physical Chemistry B*, vol. 108, no. 32, pp. 12061–12072, 2004.

[101] M. K. Ridley, T. Hiemstra, W. H. van Riemsdijk, and M. L. Machesky, "Inner-sphere complexation of cations at the rutile–water interface: A concise surface structural interpretation with the CD and MUSIC model," *Geochimica et Cosmochimica Acta*, vol. 73, no. 7, pp. 1841–1856, Apr. 2009.

[102] C.-C. Chen and K. F. Hayes, "X-ray absorption spectroscopy investigation of aqueous Co (II) and Sr (II) sorption at clay–water interfaces," *Geochimica et Cosmochimica Acta*, vol. 63, no. 19, pp. 3205–3215, 1999.

[103] R. H. Parkman, J. M. Charnock, F. R. Livens, and D. J. Vaughan, "A study of the interaction of strontium ions in aqueous solution with the surfaces of calcite and kaolinite," *Geochimica et cosmochimica acta*, vol. 62, no. 9, pp. 1481–1492, 1998.

[104] M. G. Mac Naughton and R. O. James, "Adsorption of aqueous mercury (II) complexes at the oxide/water interface," *Journal of Colloid and Interface Science*, vol. 47, no. 2, pp. 431–440, 1974.

[105] D. G. Kinniburgh, J. K. Syers, and M. L. Jackson, "Specific adsorption of trace amounts of calcium and strontium by hydrous oxides of iron and aluminum," *Soil Science Society of America Journal*, vol. 39, no. 3, pp. 464–470, 1975.

[106] U. Schwertmann and R. M. Cornell, "Methods of characterization," *Iron Oxides in the Laboratory: Preparation and Characterization*, pp. 27–54, 2000.

[107] U. Schwertmann, P. Cambier, and E. Murad, "Properties of goethites of varying crystallinity,"

Clays and Clay Minerals, vol. 33, no. 5, pp. 369–378, 1985.
[108] D. Peak, R. Ford, and D. Sparks, "An in Situ ATR-FTIR Investigation of Sulfate Bonding Mechanisms on Goethite.," *Journal of colloid and interface science*, vol. 218, no. 1, pp. 289–299, Oct. 1999.
[109] A. Vieira, *Surface complexation modeling of Pb (II), Cd (II) and Se (IV) onto iron hydroxides in single and bisolute systems*, no. Ii. 2007.
[110] J. E. Mangold, "Predicting Ion Adsorption onto the Iron Hydroxide Goethite in Single and Multi-Solute Systems," 2013.
[111] J. W. Bowden, S. Nagarajah, N. J. Barrow, A. M. Posner, and J. P. Quirk, "Describing the adsorption of phosphate, citrate and selenite on a variable-charge mineral surface," *Soil Research*, vol. 18, no. 1, pp. 49–60, 1980.
[112] W. Zeltner and M. A. Anderson, "Surface charge development at the goethite/aqueous solution interface: effects of CO2 adsorption," *Langmuir*, no. 14, pp. 469–474, 1988.
[113] R. P. J. J. Rietra, T. Hiemstra, and W. H. van Riemsdijk, "Electrolyte Anion Affinity and Its Effect on Oxyanion Adsorption on Goethite.," *Journal of colloid and interface science*, vol. 229, pp. 199–206, 2000.
[114] M. Talebi Atouei, R. Rahnemaie, E. Goli Kalanpa, and M. H. Davoodi, "Competitive adsorption of magnesium and calcium with phosphate at the goethite water interface: Kinetics, equilibrium and CD-MUSIC modeling," *Chemical Geology*, vol. 437, pp. 19–29, 2016.
[115] S. N. Stokes, "Diffuse layer modeling on iron oxides: Single and multi-solute systems on ferrihydrite and granular ferric hydroxide," 2009.
[116] F. Gaboriaud and J. J. Ehrhardt, "Effects of different crystal faces on the surface charge of colloidal goethite (a-FeOOH) particles: An experimental and modeling study," *Geochimica et Cosmochimica Acta*, vol. 67, no. 5, pp. 967–983, 2003.
[117] V. Barron and J. Torrent, "Surface Hydroxyl Configuration of Various Crystal Faces of Hematite and Goethite," *Journal of Colloid and Interface Science*, vol. 177, no. 2, pp. 407–410, 1996.
[118] T. Hiemstra and W. H. Van Riemsdijk, "A surface structural model for ferrihydrite I: Sites related to primary charge, molar mass, and mass density," *Geochimica et Cosmochimica Acta*, vol. 73, no. 15, pp. 4423–4436, 2009.
[119] D. E. Yates, "The structure of the oxide/aqueous electrolyte interface," University of Melbourne, Australia, 1975.
[120] H. Wijnja and C. P. Schulthess, "ATR–FTIR and DRIFT spectroscopy of carbonate species at the aged γ-Al 2 O 3/water interface," *Spectrochimica Acta Part A: Molecular and Biomolecular Spectroscopy*, vol. 55, no. 4, pp. 861–872, 1999.
[121] J. P. Gustafsson, "Visual MINTEQ version 3.0 beta. Royal Institute of technology, department of Land and Water Resources Engineering, Stockholm, Sweden." 2010.
[122] A. L. Herbelin and J. C. Westall, "FITEQL 4.0 User's Manual," *Dept Chemistry, Oregon State University*, 1999.
[123] G. A. Waychunas, B. A. Rea, C. C. Fuller, and J. A. Davis, "Surface chemistry of ferrihydrite: Part 1. EXAFS studies of the geometry of coprecipitated and adsorbed arsenate," *Geochimica et Cosmochimica Acta*, vol. 57, no. 10, pp. 2251–2269, May 1993.
[124] G. Sposito, "Surface-reactions in natural aqueous colloidal systems," *Chimia*, vol. 43, no. 6, pp. 169–176, 1989.
[125] C. J. Chisholm-Brause, P. A. O'Day, G. E. J. Brown, and G. A. Parks, "Evidence for multinuclear metal-ion complexes at solid/water interfaces from X-ray absorption spectroscopy," *Nature*, vol. 348, no. 6301, pp. 528–531, 1990.
[126] L. J. Criscenti and D. A. Sverjensky, "The role of electrolyte anions (ClO 4-, NO 3-, and Cl-) in divalent metal (M 2+) adsorption on oxide and hydroxide surfaces in salt solutions," *American Journal of Science*, vol. 299, no. 10, pp. 828–899, 1999.
[127] A. Manceau, M. Schlegel, K. L. Nagy, and L. Charlet, "Evidence for the formation of trioctahedral clay upon sorption of Co2+ on quartz," *Journal of Colloid and Interface Science*, vol. 220, no. 2,

pp. 181–197, 1999.
[128] R. M. Cornell and R. Giovanoli, “Factors that govern the formation of multi-domainic goethites,” *Clays and Clay Minerals*, vol. 34, no. 5, pp. 557–564, 1986.
[129] R. M. Cornell and U. Schwertmann, “The iron oxide,” *VCH, New York*, p. 377, 1996.
[130] P. G. Weidler, T. Schwinn, and H. E. Gaub, “Vicinal faces on synthetic goethite observed by atomic force microscopy,” *Clays and clay minerals*, vol. 44, no. 4, pp. 437–442, 1996.
[131] P. Venema, T. Hiemstra, and P. G. Weidler, “Intrinsic proton affinity of reactive surface groups of metal (hydr) oxides: Application to iron (hydr) oxides,” *Journal of Colloid and Interface Science*, vol. 198, no. 198, pp. 282–295, 1998.
[132] L. Spadini, A. Manceau, P. W. Schindler, and L. Charlet, “Structure and Stability of Cd2+ Surface Complexes on Ferric Oxides: 1. Results from EXAFS Spectroscopy,” *Journal of Colloid and Interface Science*, vol. 168, pp. 73–86, 1994.
[133] S. R. Randall, D. M. Sherman, K. V. Ragnarsdottir, and C. R. Collins, “The mechanism of cadmium surface complexation on iron oxyhydroxide minerals,” *Geochimica et Cosmochimica Acta*, vol. 63, no. 19–20, pp. 2971–2987, 1999.
[134] C. R. Collins, D. M. Sherman, and K. V. Ragnarsdottir, “Surface complexation of Hg2+ on goethite: Mechanism from EXAFS spectroscopy and density functional calculations,” *Journal of colloid and interface science*, vol. 219, no. 2, pp. 345–350, 1999.
[135] J. R. Bargar, G. E. Brown, and G. A. Parks, “Surface complexation of Pb (II) at oxide-water interfaces: I. XAFS and bond-valence determination of mononuclear and polynuclear Pb (II) sorption products on aluminum oxides,” *Geochimica et Cosmochimica Acta*, vol. 61, no. 13, pp. 2617–2637, 1997.
[136] J. R. Bargar, G. E. Brown, and G. A. Parks, “Surface complexation of Pb (II) at oxide-water interfaces: II. XAFS and bond-valence determination of mononuclear Pb (II) sorption products and surface functional groups on iron oxides,” *Geochimica et Cosmochimica Acta*, vol. 61, no. 13, pp. 2639–2652, 1997.
[137] J. R. Bargar, S. N. Towle, G. E. Brown, and G. A. Parks, “XAFS and bond-valence determination of the structures and compositions of surface functional groups and Pb (II) and Co (II) sorption products on single-crystal α-Al2O3,” *Journal of Colloid and Interface Science*, vol. 185, no. 2, pp. 473–492, 1997.
[138] J. D. Ostergren, G. E. Brown, G. A. Parks, and P. Persson, “Inorganic ligand effects on Pb (II) sorption to goethite (α-FeOOH): II. Sulfate,” *Journal of Colloid and Interface Science*, vol. 225, no. 2, pp. 483–493, 2000.
[139] S. Fendorf, M. J. Eick, P. Grossl, and D. L. Sparks, “Arsenate and chromate retention mechanisms on goethite. 1. Surface structure,” *Environmental science & technology*, vol. 31, no. 2, pp. 315–320, 1997.
[140] M. Villalobos and A. Pérez-Gallegos, “Goethite surface reactivity: A macroscopic investigation unifying proton, chromate, carbonate, and lead(II) adsorption,” *Journal of Colloid and Interface Science*, vol. 326, no. 2, pp. 307–323, 2008.
[141] T. Hiemstra and W. H. Van Riemsdijk, “Effect of different crystal faces on experimental interaction force and aggregation of hematite,” *Langmuir*, vol. 15, no. 23, pp. 8045–8051, 1999.
[142] D. E. Yates, F. Grieser, R. Cooper, and T. W. Healy, “Tritium exchange studies on metal oxide colloidal dispersions,” *Australian Journal of Chemistry*, vol. 30, no. 8, pp. 1655–1660, 1977.
[143] R. H. Parkman, J. M. Charnock, N. D. Bryan, F. R. Livens, and D. J. Vaughan, “Reactions of copper and cadmium ions in aqueous solution with goethite, lepidocrocite, mackinawite, and pyrite,” *American Mineralogist*, vol. 84, no. 3, pp. 407–419, 1999.
[144] G. Ona-Nguema, G. Morin, F. Juillot, G. Calas, and G. E. Brown, “EXAFS analysis of arsenite adsorption onto two-line ferrihydrite, hematite, goethite, and lepidocrocite,” *Environmental science & technology*, vol. 39, no. 23, pp. 9147–9155, 2005.